PLOS | GENETICS

RESEARCH ARTICLE

A Model of Compound Heterozygous, Loss-of-Function Alleles Is Broadly Consistent with Observations from Complex-Disease GWAS Datasets

Jaleal S. Sanjak[1,2]*, Anthony D. Long[1,2], Kevin R. Thornton[1,2]*

1 Department of Ecology and Evolutionary Biology, University of California, Irvine, Irvine, California, USA, **2** Center for Complex Biological Systems, University of California, Irvine, Irvine, California, USA

* jsanjak@uci.edu (JSS); krthornt@uci.edu (KRT)

OPEN ACCESS

Citation: Sanjak JS, Long AD, Thornton KR (2017) A Model of Compound Heterozygous, Loss-of-Function Alleles Is Broadly Consistent with Observations from Complex-Disease GWAS Datasets. PLoS Genet 13(1): e1006573. doi:10.1371/journal.pgen.1006573

Editor: Simon Gravel, McGill University, CANADA

Received: April 18, 2016

Accepted: January 5, 2017

Published: January 19, 2017

Data Availability Statement: Our simulation code and code for downstream analyses are freely available at: http://github.com/ThorntonLab/disease_sims, http://github.com/molpopgen/buRden, http://github.com/molpopgen/fwdpy, and http://github.com/molpopgen/TennessenEAonly.

Funding: This work was supported by NIH grant R01-GM115564 to KRT. This work was supported by NIH grant R01-GM115562 to ADL. This material is based upon work supported by the National Science Foundation Graduate Research Fellowship Program under Grant No. DGE-1321846. Any

Abstract

The genetic component of complex disease risk in humans remains largely unexplained. A corollary is that the allelic spectrum of genetic variants contributing to complex disease risk is unknown. Theoretical models that relate population genetic processes to the maintenance of genetic variation for quantitative traits may suggest profitable avenues for future experimental design. Here we use forward simulation to model a genomic region evolving under a balance between recurrent deleterious mutation and Gaussian stabilizing selection. We consider multiple genetic and demographic models, and several different methods for identifying genomic regions harboring variants associated with complex disease risk. We demonstrate that the model of gene action, relating genotype to phenotype, has a qualitative effect on several relevant aspects of the population genetic architecture of a complex trait. In particular, the genetic model impacts genetic variance component partitioning across the allele frequency spectrum and the power of statistical tests. Models with partial recessivity closely match the minor allele frequency distribution of significant hits from empirical genome-wide association studies without requiring homozygous effect sizes to be small. We highlight a particular gene-based model of incomplete recessivity that is appealing from first principles. Under that model, deleterious mutations in a genomic region partially fail to complement one another. This model of gene-based recessivity predicts the empirically observed inconsistency between twin and SNP based estimated of dominance heritability. Furthermore, this model predicts considerable levels of unexplained variance associated with intralocus epistasis. Our results suggest a need for improved statistical tools for region based genetic association and heritability estimation.

Author Summary

Gene action determines how mutations affect phenotype. When placed in an evolutionary context, the details of the genotype-to-phenotype model can impact the maintenance of genetic variation for complex traits. Likewise, non-equilibrium demographic history may

opinions, findings, and conclusions or recommendations expressed in this material are those of the authors and do not necessarily reflect the views of the National Science Foundation. The funders had no role in study design, data collection and analysis, decision to publish, or preparation of the manuscript.

Competing Interests: The authors have declared that no competing interests exist.

affect patterns of genetic variation. Here, we explore the impact of genetic model and population growth on distribution of genetic variance across the allele frequency spectrum underlying risk for a complex disease. Using forward-in-time population genetic simulations, we show that the genetic model has important impacts on the composition of variation for complex disease risk in a population. We explicitly simulate genome-wide association studies (GWAS) and perform heritability estimation on population samples. A particular model of gene-based partial recessivity, based on allelic non-complementation, aligns well with empirical results. This model is congruent with the dominance variance estimates from both SNPs and twins, and the minor allele frequency distribution of GWAS hits.

Introduction

Risk for complex diseases in humans, such as diabetes and hypertension, is highly heritable yet the causal DNA sequence variants responsible for that risk remain largely unknown. Genome-wide association studies (GWAS) have found many genetic markers associated with disease risk [1]. However, follow-up studies have shown that these markers explain only a small portion of the total heritability for most traits [2, 3].

There are many hypotheses which attempt to explain the 'missing heritability' problem [2–5]. Genetic variance due to epistatic or gene-by-environment interactions is difficult to identify statistically because of, among other reasons, increased multiple hypothesis testing burden [6, 7], and could artificially inflate estimates of broad-sense heritability [8]. Well-tagged intermediate frequency variants may not reach genome-wide significance in an association study if they have smaller effect sizes [9, 10]. One appealing verbal hypothesis for this 'missing heritability' is that there are rare causal alleles of large effect that are difficult to detect [4, 11, 12]. These hypotheses are not mutually exclusive, and it is probable that a combination of models will be needed to explain all heritable disease risk [13].

The standard GWAS attempts to identify genetic polymorphisms that differ in frequency between cases and controls. A complementary approach is to estimate the heritability explained by genotyped (and imputed) markers (SNPs) under different population sampling schemes [14, 15]. Stratifying markers by minor allele frequency (MAF) prior to performing SNP-based heritability estimation allows the partitioning of genetic variation across the allele frequency spectrum to be estimated [16], which is an important summary of the genetic architecture of a complex trait [16–23]. This approach has inferred a contribution of rare alleles to genetic variance in both human height and body mass index (BMI) [16], consistent with theoretical work showing that rare alleles will have large effect sizes if fitness effects and trait effects are correlated [18, 20–25]. Yet, simulations of causal loci harboring multiple rare variants with large additive effects predict an excess of low-frequency significant markers relative to empirical findings [4, 26].

SNP-based heritability estimates have concluded that there is little missing heritability for height and BMI, and that the causal loci simply have effect sizes that are too small to reach genome-wide significance under current GWAS sample sizes [14, 16]. Further, extensions to these methods decompose genetic variance into additive and dominance components and find that dominance variance is approximately one fifth of the additive genetic variance on average across seventy-nine complex traits [27]. When taken into account together with results from GWAS, these observations can be interpreted as evidence that the genetic architecture of human traits is best-explained by a model of small additive effects. However, a recent large

twin study found a substantial contribution of dominance variance for fourteen out of eighteen traits [28]. The reason for this discrepancy in results remains unclear. One possibility is a statistical artifact; for example, twin studies may be prone to mistakenly infer non-additive effects when none exist. Another possibility, which we return to later, is that this apparently contradictory results are expected under a different model of gene action.

The design, analysis, and interpretation of GWAS are heavily influenced by the "standard model" of quantitative genetics [29]. This model assigns an effect size to a mutant allele, but formally makes no concrete statement regarding the molecular nature of the allele. Early applications of this model to the problem of human complex traits include Risch's work on the power to detect causal mutations [30, 31] and Pritchard's work showing that rare alleles under purifying selection may contribute to heritable variation in complex traits [17]. When applied to molecular data, such as SNP genotypes in a GWAS, these models treat the SNPs themselves as the loci of interest. For example, influential power studies informing the design of GWAS assign effect sizes directly to SNPs and assume Risch's model of multiplicative epistasis [32]. Similarly, the single-marker logistic regression used as the primary analysis of GWAS data typically assumes an additive or recessive model at the level of individual SNPs [33]. Finally, recent methods designed to estimate the heritability of a trait explained by genotyped markers assigns additive and dominance effects directly to SNPs [14, 16, 27, 34]. Naturally, the results of such analyses are interpreted in light of the assumed model of gene action.

A weakness of the multiplicative epistasis model [30, 31] when applied to SNPs is that the concept of a gene, defined as a physical region where loss-of-function mutations have the same phenotype [35], is lost. Specifically, under the standard model, the genetic concept of a failure to complement is a property of SNPs and not "gene regions" (see [36] for a detailed discussion of this issue). We have recently introduced an alternative model of gene action, one in which risk mutations are unconditionally deleterious and fail to complement at the level of a "gene region" [36]. This model, influenced by the standard operational definition of a gene [35], gives rise to the sort of allelic heterogeneity typically observed for human Mendelian diseases [37], and to a distribution of GWAS "hit" minor allele frequencies [4, 26] consistent with empirical results [36]. In this article, we explore this "gene-based" model under more complex demographic scenarios as well as its properties with respect to the estimation of variance components using SNP-based approaches [34] and twin studies. We also compare this model to the standard models of strictly additive co-dominant effects, and multiplicative epistasis with dominance.

We further explore the power of several association tests to detect a causal gene region under each genetic and demographic model. We find significant heterogeneity in the performance of burden tests [36, 38, 39] across models of the trait and demographic history. We find that population expansion reduces the power to detect causal gene-regions due to an increase in rare variation, in agreement with work by [22, 23]. The behavior of the tests under different models provides us with insight as to the circumstances in which each test is best suited.

In total, our results show that modeling gene action is key to modeling GWAS, and thus plays an important role in both the design and interpretation of such studies. Further, the model of gene-based recessivity best explains the differences between estimates of additive and dominance variance components from SNP-based methods [27] and from twin studies [28] and is consistent with the distribution of frequencies of significant associations in GWAS [4, 26]. Further, the genetic model plays a much more important role than the demographic model, which is expected based on previous work on additive models showing that the genetic load is approximately unaffected by changes in population size over time, [21, 22]. Consistent with recent work by [23], we find that rapid population growth in the recent past increases the contribution of rare variants to total genetic variance. However, we show here that different

models of gene action are qualitatively different with respect to the partitioning of genetic variance across the allele frequency spectrum. We also show that these conclusions hold under the more complex demographic models that have been proposed for human populations [21, 40].

Results and Discussion

The models

As in [36],we simulate a 100 kilobase region of human genome, contributing to a complex disease phenotype and fitness. The region evolves forward in time subject to neutral and deleterious mutation, recombination, selection, and drift. To perform genetic association and heritability estimation studies *in silico*, we need to impose a trait onto simulated individuals. In doing so, we introduce strong assumptions about the molecular underpinnings of a trait and its evolutionary context.

How does the molecular genetic basis of a trait under natural selection influence population genetic signatures in the genome? This question is very broad, and therefore it was necessary to restrict ourselves to a small subset of molecular and evolutionary scenarios. We analyzed a set of approaches to modeling a single gene region experiencing recurrent unconditionally-deleterious mutation contributing to a quantitative trait subject to Gaussian stabilizing selection. The expected fitness effect of a mutation is always deleterious because trait effects are sampled from an exponential distribution. Therefore, we do not allow for compensatory mutations that may occur in more general models of stabilizing selection. Specifically, we studied three different genetic models and two different demographic models, holding the fitness model as a constant. Parameters are briefly described in Table 1.

We implemented three disease-trait models of the phenotypic form $P = G + E$. G is the genetic component, and $E = N(0, \sigma_e^2)$ is the environmental noise expressed as a Gaussian random variable with mean 0 and variance σ_e^2. In this context, σ_e^2 should be thought of as both the contribution from the environment and from the remaining genetic variance at loci in linkage equilibrium with the simulated 100kb region. The genetic models are named the additive co-dominant (AC) model, multiplicative recessive (Mult. recessive; MR) model and the gene-based recessive (GBR) model. The MR model has a parameter, h, that controls the degree of

Table 1. Description of parameters used in the models.

Parameter	Description
N	Population size
P	Phenotype
P_{opt}	Optimum phenotype
G	Genetic contribution to phenotype
E	Environmental contribution to phenotype
λ	Mean and standard deviation of trait effects
c_i	Specific trait effect of site i
h	Dominance coefficient for trait effects
w	Fitness, based on Gaussian function
σ_s^2	The total inverse selection intensity
σ_e^2	Environmental variance
V_A	Additive genetic variance
V_D	Dominance genetic variance
V_G	Genetic variance
$V_{A;q \leq x}$	Additive variance explained by variance below frequency q

doi:10.1371/journal.pgen.1006573.t001

recessivity; we call this model the complete MR (cMR) when $h = 0$ and the incomplete MR (iMR) when $0 \leq h \leq 1$. Here, $h = 1$ corresponds to co-dominance, which is different from the typical formulation used when modeling the fitness effects of mutations directly. It is also important to note that here recessivity is being defined in terms of phenotypic effects; this may be unusual for those more accustomed to dealing directly with recessivity for fitness effects. An idealized relationship between dominance for fitness effects and trait effects of a mutation on an unaffected genetic background is shown in S15 Fig.

The critical conceptual difference between recessive models is whether dominance is a property of a locus (nucleotide/SNP) in a gene or the gene overall. Mathematically, this amounts to whether one first determines diploid genotypes at sites (and then multiplies across sites to get a total genetic effect) or calculates a score for each haplotype (the maternal and paternal alleles). For completely co-dominant models, this distinction is irrelevant, however for a model with arbitrary dominance one needs to be more specific. As an example, imagine a compound heterozygote for two biallelic loci, i.e. genotype Ab/aB. In the case of traditional multiplicative recessivity the compound heterozygote is wild type for both loci and therefore wild-type over all; this implies that these loci are in different genes (or independent functional units of the same gene) because the mutations are complementary. However, in the case of gene-based recessivity [36], neither haplotype is wild-type and so the individual is not wild-type; the failure of mutant alleles to complement defines these loci as being in the same gene [35].

For a diploid with m_i causative mutations on the i^{th} haplotype, we may define the additive model as

$$G_{AC} = \sum_{i=1}^{2} \sum_{j=1}^{m_i} c_{i,j}, \tag{1}$$

where $c_{i,j}$ is the effect size of the j^{th} mutation on the i^{th} haplotype. Each $c_{i,j}$ is sampled from an exponential distribution with mean of λ, to reflect unconditionally deleterious mutation. In other words, when a new mutation arises its effect c is drawn from an exponential distribution, and remains constant throughout its entire sojourn in the population.

The GBR model is the geometric mean of the sum of effect sizes on each haplotype [36]. We sum the causal mutation effects on each allele (paternal and maternal) to obtain a haplotype score. We then take the square root of the product of the haplotype scores to determine the total genetic value of the diploid.

$$G_{GBR} = \sqrt{\sum_{j=1}^{m_1} c_{1,j} \times \sum_{j=1}^{m_2} c_{2,j}} \tag{2}$$

Finally, the MR model depends on the number of positions for which a diploid is heterozygous (m_{Aa}) or homozygous (m_{aa}) for causative mutations,

$$G_{MR} = \left(\prod_{j=1}^{m_{Aa}} (1 + hc_j) \right) \left(\prod_{j=1}^{m_{aa}} (1 + 2c_j) \right) - 1. \tag{3}$$

Thus, $h = 0$ is a model of multiplicative epistasis with complete recessivity (cMR), and $h = 1$ closely approximates the additive model when effect sizes are small.

Here, phenotypes are subject to Gaussian stabilizing selection with an optimum at zero and standard deviation of $\sigma_s = 1$ such that the fitness, w, of a diploid is proportional to a Gaussian

function [41].

$$w = e^{-\frac{p^2}{2\sigma_s^2}} \quad (4)$$

The AC and MR models draw no distinction between a "mutation" and a "gene" (as discussed in [36]). The GBR is also a recessive model, but recessivity is at the level of a *haplotype* (or allele) and is not an inherent property of individual mutations (see [36] for motivation of this model). Viewed in light of the traditional AC and MR models, the recessivity of a *site* in the GBR model is a function of the local genetic background on which it is found. Based on several qualitative comparisons we find that the GBR model is approximated by iMR models with $0.1 \leq h \leq 0.25$. However, no specific iMR model seems to match well in all aspects. The demographic models are that of a constant sized population (no growth) and rapid population expansion (growth).

The use of the MR model is inspired by Risch's work [30, 31], linking a classic evolutionary model of multiple loci interacting multiplicatively [42, 43] to the the genetic epidemiological parameter relative risk. Risch and Merikangas [44] used this model to calculate the power to detect causal risk variants as a function of their frequency and effect size. Pritchard extended Risch's model to consider a trait explicitly as a product of the evolutionary process [17]. Pritchard's work demonstrated that the equilibrium frequency distribution suggested an important role for rare deleterious mutations when a trait evolves in a constant sized, randomly mating population with recurrent mutation and constant effect sizes. However, multiplicative epistasis is only one model of gene action. Exploring the effect of different genotype-to-phenotype models on the population and quantitative genetic properties of complex traits is the focus of the current work.

Additive and dominance genetic variance in the population

The amount of narrow sense heritability, $h^2 = (V_A)/(V_P)$, explained by variants across the frequency spectrum is directly related to the effect sizes of those variants [29]. Thus, this measure is an important predictor of statistical power of GWAS and should inform decisions about study design and analysis [45]. Empirically, SNP-based estimates of heritability have inferred negligible dominance variance underlying most quantitative traits [27]. We have a particular interest in the amount of additive variance, V_A, that is due to rare alleles and how much of genetic variance, V_G, is attributable to V_A under different recessive models.

We follow the approach of [21], by calculating the cumulative percent of V_G explained by the additive effects of variants less than or equal to frequency x, $(V_{A;q \leq x})/(V_G)$. The product of this ratio and broad-sense heritability is an estimate of the narrow-sense heritability, h^2. This calculation is a population-wide equivalent to a SNP-based estimate of heritability in a population sample. In addition we calculate the same distribution for dominance effects $(V_{D;q \leq x})/(V_G)$ using the orthogonal model of [27]. Methods based on summing effect sizes [29] or the site frequency spectrum [21] would not apply to the GBR model, because the effect of a variant is not independent of other variants (*e.g.*, there is intralocus epistasis). Therefore, we resort to a regression-based approach, where we regress the genotypes of the population onto the total genetic value as defined in our disease trait models (see Material and Methods). In the limit of Hardy-Weinberg and linkage equilibrium, the regression estimates are equivalent to standard quantitative genetic estimates [29] (S14 Fig). For consistency, we applied the regression approach to all models. Overall, these distributions are substantially different across genetic models, demographic scenarios and model parameters (Fig 1).

Under the AC model, all of V_G is explained by additive effects if all variants are included in the calculation; in Fig 1 the solid variance curves reach unity in the AC panel. Low frequency

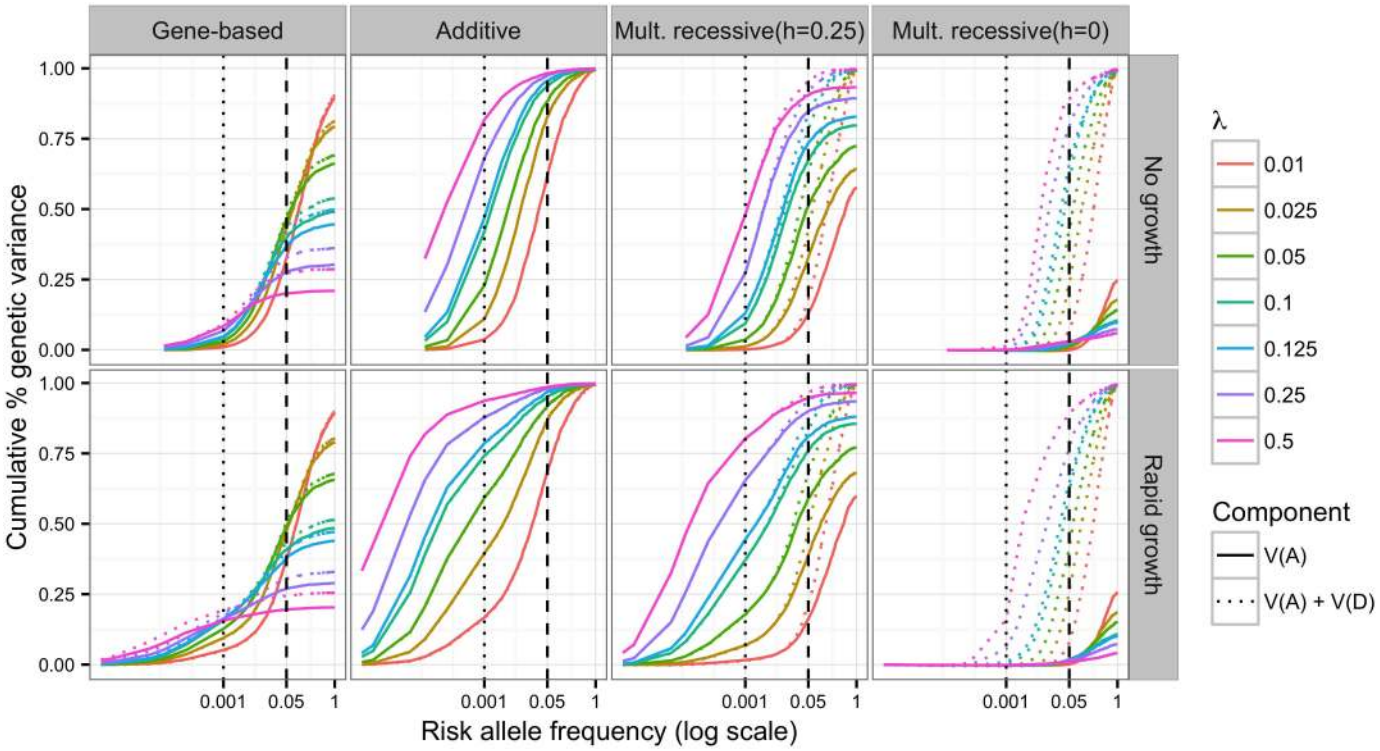

Fig 1. Variance explained over allele frequency. The cumulative additive and dominance genetic variance which can be explained by markers whose frequencies, q, are $\leq x$. Each color represents a different value of λ: the mean effects size of a new deleterious mutation. Shown here are the gene-based (GBR), additive co-dominant (AC), incomplete multiplicative recessive (Mult. recessive ($h = 0.25$); iMR) and complete multiplicative recessive (Mult. recessive ($h = 0$);cMR) models. Solid lines show the additive variance alone and dotted lines show the combined additive and dominance variance. All data shown are for models where $H^2 \sim 0.08$. These particular results are robust to changes H^2 when V_G is not changed, as is the case here. The additive and dominance genetic variance is estimated by the adjusted r^2 of the regression of all markers (and their corresponding dominance encoding) with $q \leq x$ onto total genotypic value (see methods for details); data are displayed as the mean of 250 simulation replicates. The vertical dotted and dashed lines correspond to the $q = 0.001$ and $q = 0.05$, respectively. The curves under no growth appear to be truncated with respect to rapid growth because the range of the x-axis differs between growth and no growth (minimum $q = 1/2N$).

doi:10.1371/journal.pgen.1006573.g001

and rare variants ($q < 0.01$) explain a large portion of narrow sense heritability (26%–95%) even in models without rapid population expansion. Further, the variance explained at any given frequency threshold increases asymptotically to unity as a function of increasing λ (S4 Fig). While the total heritability of a trait in the population is generally insensitive to population size changes (S1 Fig, see also [21, 22, 46]), rapid population growth increases the fraction of additive genetic variation due to rare alleles (Fig 1).

Here, increasing λ corresponds to stronger selection against causative mutations, due to their increased average effect size. Recent work by Zuk et al. [24], takes a similar approach and relates the allele frequency distribution directly to design of studies for detecting the role of rare variants. However, our findings contrast with those of Zuk et al. [24] and agree with those of Lohmueller [22], in that we predict that population expansion will substantially increase the heritability, or portion of genetic variance, that is due to rare variants. Our results under the AC model agree with those of Simons et al. [21], in that we find that increasing strength of selection, increasing λ in our work, increases the contribution to heritability of rare variants. However, under the GBR model and the cMR model the distribution of genetic variance over risk allele frequency as function λ is non-monotonic (Fig 1 and S4 Fig).

For all recessive models, we find that total V_A is less than V_G (Fig 1). For the MR models, all additional genetic variation is explained by the dominance variance component; in Fig 1 the

dotted variance curves reach unity in the MR panels. As expected, genetic variation under the MR model with partial recessivity ($h = 0.25$) is primarily additive [29, 47], whereas V_G under the cMR model ($h = 0$) is primarily due to dominance. The GBR model shows little dominance variance and is the only model considered here for which the total V_G explained by V_A+V_D is less than the true V_G for all λ. This can be clearly seen in Fig 1 where the dotted curves do not reach unity in the GBR panel. These observations concerning the GBR model are consistent with the finding of [27] that dominance effects of SNPs do not contribute significantly to the heritability for complex traits.

Under the GBR model, large trait values are usually due to compound heterozygote genotypes (*e.g.*, *Ab*/*aB*, where A and B represent different sites in the same gene) [36]. Therefore, the recessivity is at the level *of the gene region* while the typical approach to estimating V_A and V_D assigns effect sizes and dominance to individual mutations. Thus, compound heterozygosity, which is commonly observed for Mendelian diseases (see [36] and references therein) would be interpreted as variation due to *interactions* (epistasis) between risk variants. Importantly, the GBR model assumes that such interactions should be local, occurring amongst causal mutations in the same locus. While the GBR model is reflective of the original definition of a gene in which recessive mutations fail to complement, we emphasize that this does not imply that mutations are necessarily exomic. The GBR model is of a general genomic region in which mutations act locally in *cis* to disrupt the function of that region with respect to a phenotype.

The increase in the number of rare alleles due to population growth is a well established theoretical and empirical result [48–61]. The exact relationship between rare alleles [4, 17, 26, 62, 63], and the demographic and/or selective scenarios from which they arose [21, 22, 64], and the genetic architecture of common complex diseases in humans is an active area of research. An important parameter dictating the relationships between demography, natural selection, and complex disease risk is the degree of correlation between a variants effect on the disease trait and its effect on fitness [18, 20–22]. In our simulations, we do not impose an explicit degree of correlation between the phenotypic and fitness effects of a variant. Rather, this correlation is context dependent, varying according to the current genetic burden of the population, the genetic background in which the variant is present and random environmental noise. However, if we re-parameterized our model in terms of [18], then we would have $\tau \leq 0.5$ (Gaussian function is greater than or equal to its quadratic approximation), which is consistent with recent attempts at estimating that parameter [20, 65]. Our approach is reflective of weak selection acting directly on the complex disease phenotype, but the degree to which selection acts on genotype is an outcome of the model. While the recent demographic history has little effect on key mean values such as broad-sense heritability of a trait or population genetic burden (S1 and S3 Figs), the structure of the individual components in the population which add up to those mean values varies considerably. The specific predictions with respect to the composition of the populations varies drastically across different modeling approaches. It is therefore necessary to carefully consider the structure of a genetic model in a simulation study.

The conclusions reached here also hold when we consider more complex demographic scenarios relevant to human populations. Under the demographic model for European populations from [40], the additive and GBR models show the same behavior as in Fig 1 (S17 Fig). At all key time points where population size changes, $V_A = V_G$ for the additive model, and the variance explained by rare mutations depends primarily on λ (S17 Fig). For the GBR model, $V_A < V_G$ (as in Fig 1), and plateaus at the same ratio V_A/V_G for all time points except immediately after the bottleneck, which results in a short-lived increase in V_A/V_G that is undetectable by the time growth begins (S17 Fig). All recessive models (GBR, iMR and cMR) may show a transient increase in total V_G after the bottleneck, depending on the value of λ (S18 Fig). However, the

GBR and iMR models with $h > 0.25$ showed a return to constant population size levels by the final time point. The changes in V_A and V_G under recessive models is likely due to the transfer of non-additive variation into V_A during a bottleneck, which has been studied thoroughly in the theoretical literature [66, 67]. As in Fig 1, the genetic model, and not the demographic details, drive the relationship between mutation frequency and additive genetic variance. In agreement with existing literature, site based recessive models show complex dynamics during bottlenecks and population expansion (S18 and S19 Figs). However, with respect to load, the GBR model behaves more like a codominant model and is largely insensitive to changes in population size(S18 and S19 Figs). Thus, complex traits evolving under the GBR model are not expected to show large differences in load between extant human populations.

Estimating additive and dominance variance from population samples

The previous section shows that the relationship between genetic variance and allele frequency in the entire population strongly depends on the genetic model. Recent estimates of variance components from large population samples of unrelated individuals have inferred that dominance variance (V_D) is negligible for most traits [27]. However, a recent study of more than 10^4 Swedish twins and 18 traits obtained a contradictory result, inferring significant non-additive variance for most traits, which was interpreted as V_D [68]. In this section, we show that this apparent inconsistency is expected under certain models of gene action.

We applied GREMLd, MAF-stratified GREMLd (MS-GREMLd), and MAF-stratified Haseman-Elston regression (see Methods for details). We found MS-GREMLd to be numerically unstable on our simulated data, and thus we present results for non-MS-stratified GREMLd. The numerical stability issues likely resulted from some combination of small number of SNPs per region ($\mathcal{O}(1000)$), low total V_G in a region, or high variance in effect sizes across causal mutations [69]. Further, for large λ, where V_G is primarily due to rare alleles (Fig 1), heritability in a sample may not reflect heritability in the entire population (S13 Fig).

Fig 2 shows the GREMLd additive and dominance heritability estimates, as compared to the respective population value, over λ. Under the cMR model ($h = 0$), the dominance component is much larger than the additive component as predicted from Fig 1. When GREMLd is performed on cMR model data after removing variants with $MAF \leq 0.01$, as done in [27], the total heritability estimate (AD) is quite accurate until $\lambda \geq 0.25$ where a downward bias is observed. As anticipated, GREMLd using unfiltered data yields results with a slight upward bias [70]. However, for the iMR ($h = 0.25$) model the filtered GREMLd estimates are only accurate for $\lambda < 0.1$ reflecting the preponderance of rare causal variants for larger values of λ. Unfiltered GREMLd estimates under the iMR ($h = 0.25$) model show a slight upward bias for small values of λ, but are otherwise accurate. This shows that GREMLd is performing as expected under the site-based model for which it is designed. The MS-HE regression results are generally consistent with the GREMLd results.

The GREMLd and MS-HE estimates are accurate under the GBR model when λ is small, because most heritability is additive in that case(Fig 1). However, under the GBR model, both filtered and unfiltered GREMLd heritability estimates show downward bias when λ is large (Fig 2). The MS-HE regression results reveal a similar pattern, which indicates that the downward bias for large values of λ is not strictly due to removal of rare variants in the filtered GREMLd analysis. Instead, the bias shown for large values of λ is likely due to the presence of substantial non-additive heritability, which is not captured by the dominance effects of SNPs.

In contrast to the variance component methods, our simulated large twin studies provide approximately unbiased estimates of total heritability for large values of λ, but were biased upward for small effect sizes under the AC and GBR models (Fig 2). The variance in twin-

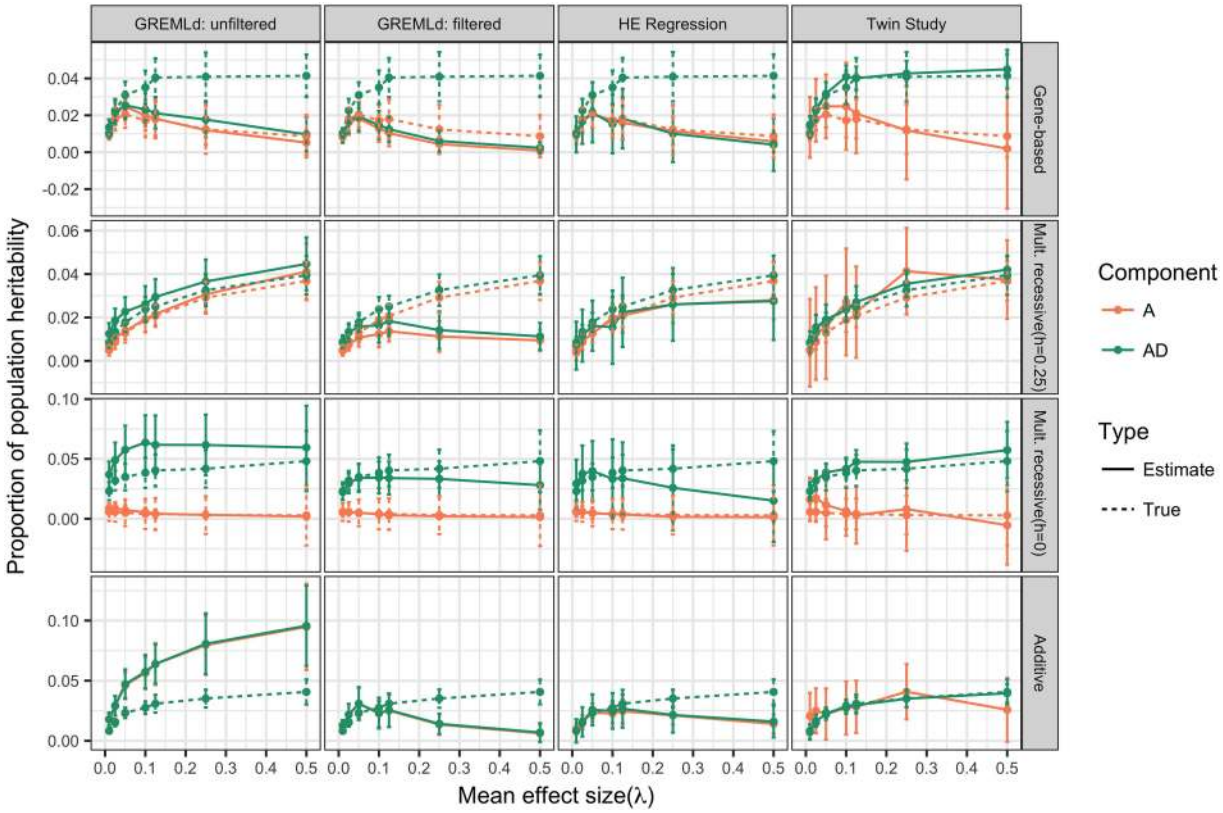

Fig 2. Heritability estimates compared to population heritability. Heritability estimates and population heritability as a function of λ: the mean effect size of a new deleterious mutation. Additive (A; orange) component of true heritability is calculated by multiplying the end point($q = 1$) of the variance curves in Fig 1 by the broad-sense heritability values summarized in S1 Fig. HE-regression and GREMLd estimates were obtained from random population samples (n = 6000). GREMLd analysis was performed in GCTA using genotype data that was either unfiltered or filtered to remove variants with MAF<0.01. Twin study estimates are directly calculated using MZ and DZ twin correlations from 64 sets of twin studies. Each study consisted of pooling 2000 MZ twin pairs and 2000 DZ twin pairs from each of 8 model replicates for a total of 64,000 individual phenotypes. Data are plotted as the median across replicate sets ± half the interquartile range. Shown are the additive co-dominant (AC), gene-based (GBR) incomplete multiplicative recessive (Mult. recessive ($h = 0.25$); iMR) and complete multiplicative recessive (Mult. recessive ($h = 0$); cMR) models.

doi:10.1371/journal.pgen.1006573.g002

study estimates was quite large, possibly because only a single locus was simulated rather than the whole genome. Formally, twin studies estimate an additive and a non-additive component of variance and interpreting the non-additive component as epistatic or dominance variance is a matter of perspective. However, the GBR model is inspired by the definition of a gene as a physical region in which recessive mutations leading to the same phenotypic outcome fail to complement [35], consistent with the allelic heterogeneity observed for human Mendelian disorders (see [36] for further discussion). Thus, the model of recessivity at the level of the gene region is picked up as non-additive variance in twin studies, but missed by variance component methods (GREML and HE regression) because the dominance in the GBR model is due to *Ab*/*aB* (compound heterozygotes) genotypes rather than *a*/*a* genotypes (homozygotes for a specific loss of function variant) assumed by variance component methods. Thus the contradictory results of applying variance component methods [27] and analysis of large twin studies [68] in order to estimate V_A and V_D may be interpreted as evidence for a model of gene action such as the GBR, which may be viewed as either recessivity at the haplotype/gene level or

intralocus epistasis at the level of causative mutations in a single gene region. Both interpretations are valid. The alternative explanation is that we must assert that one of the study designs is generating artifacts.

The genetic model affects the outcomes of GWAS

Both demography and the model of gene action affect the degree to which rare variants contribute to the genetic architecture of a trait (Fig 1). However, the different mappings of genotype to phenotype from model to model make it difficult to predict *a priori* the outcomes of GWAS under each model. Therefore, we sought to explicitly examine the performance of statistical methods for GWAS under each genetic and demographic model. We assessed the power of a single marker logistic regression to detect the gene region by calculating the proportion of model replicates in which at least one variant reached genome wide significance at $\alpha \leq 10^{-8}$ (Fig 3A). The basic logistic regression is equivalent to testing for association under the AC model. We simulated both a perfect "genotyping chip" (all markers with $MAF \geq 0.05$) and complete re-sequencing including all markers (Fig 3B).

One of the most prominent feature of Fig 3 is the curvature of power as a function of λ. This reflects the competing forces of increasing average genetic effect and decreasing average allele frequency which occurs as λ increases (S5 Fig). As λ increases, the total genetic variance explained by the locus increases until the model enters the House-of-cards [71] regime. At which point, the genetic variance is much less dependent on λ (S1 Fig). When λ is large, however, the average allele frequency does continue to decrease (S5 Fig) which drives power down.

Across all genetic models, the single marker logistic regression has less power under population expansion (Fig 3A). The loss of power is attributable to a combination of rapid growth resulting in an excess of rare variants overall [48–61], and the increasing efficacy of selection against causal variants in growing populations [21]. While complete resequencing is more powerful than a gene-chip design, the relative power gained is modest under growth (Fig 3A). Region-based rare variant association tests behave similarly with respect to population growth (Fig 3B).

There are important differences in the behavior of the examined statistical methods across genetic models. We focus first on the single marker tests (Fig 3A). For gene-chip strategies, power increases for "site-based" models as recessivity of risk variants increases (compare power for AC, iMR, and cMR models in Fig 3B). This increase in power is due to the well-known fact that recessive risk mutations are shielded from selection when rare (due to being mostly present as heterozyogtes), thus reaching higher frequencies on average (S5 Fig), and that the single-marker test is most powerful when risk variants are common [32]. Further, for the complete multiplicative-recessive model (cMR), the majority of V_G is due to common variants (Fig 1), explaining why resequencing does not increase power for this model (Fig 3A).

For single-marker tests, the GBR model predicts large gains in power under resequencing for intermediate λ (the mean trait-effect size of newly arising causal mutations), similar to the AC or iMR model. But, when λ is larger power may actually be less under the GBR model than under AC or iMR. For all models, causal mutations are more rare with increasing λ (S7 Fig). However, as a function of frequency, all V_G may be attributed to V_A or V_D in the site-specific models whereas there is increasing intralocus epistasis in the GBR model as a function of λ (Fig 1). It is well-known that the single marker test has lower power when causal mutations have low frequencies, are poorly tagged by more common SNPs, or have small main effects [32, 72].

Region-based rare variant association tests show many of the same patterns across genetic model and effect size distribution as single marker tests, but there are some interesting

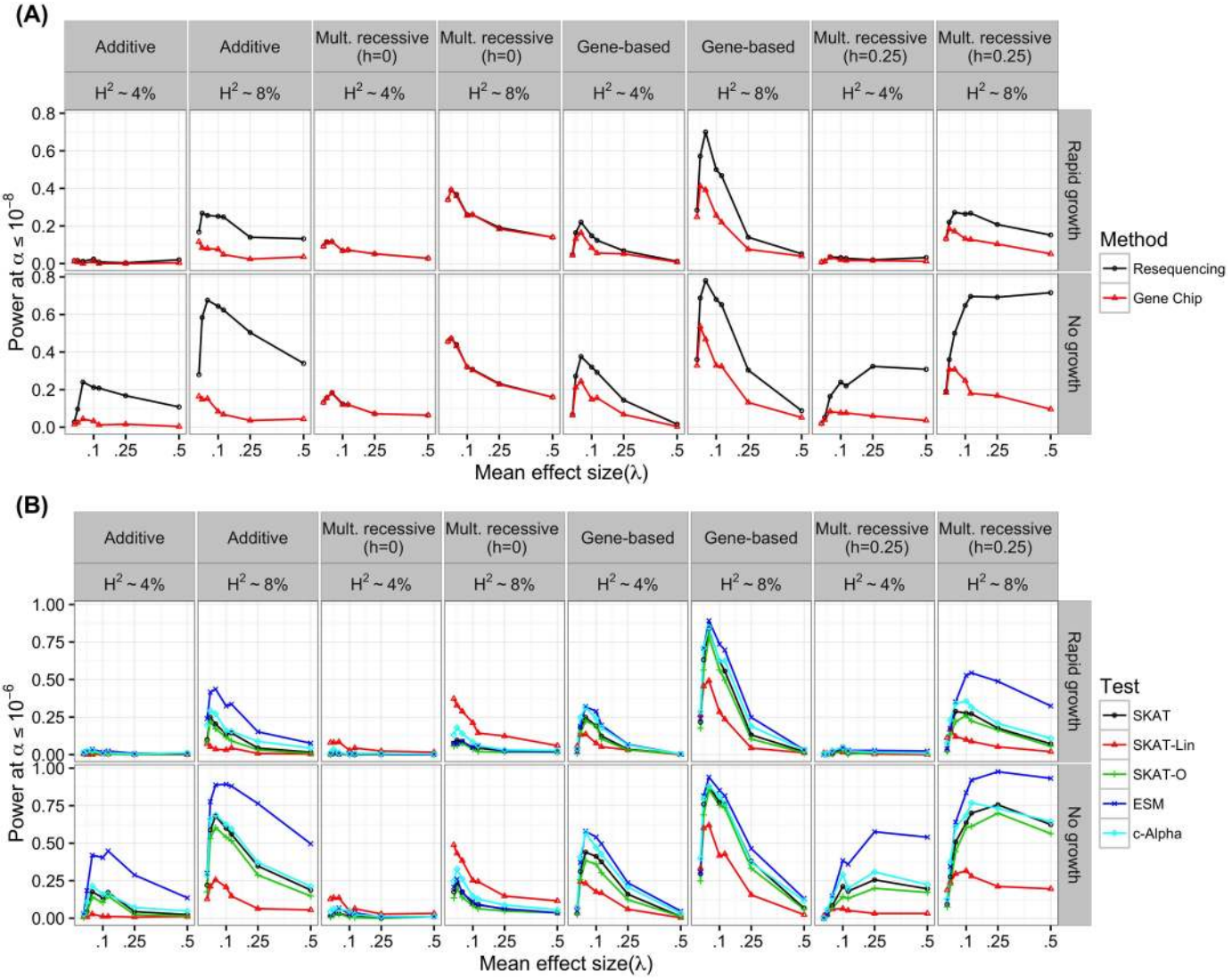

Fig 3. Power of association tests. (A) The power of a single marker logistic regression, at significance threshold of $\alpha \leq 10^{-8}$, as a function of λ: the mean effect size of a new deleterious mutation. For single marker tests we define power as the number of simulation replicates in which any single marker reaches genome wide significance. Two study designs were emulated. For the gene chip design only markers with $MAF > 0.05$ were considered and all markers were considered for the resequencing design. Genetic models shown here are the additive co-dominant (AC), gene-based (GBR), complete multiplicative site-based recessive (Mult. recessive ($h = 0$); cMR) and incomplete multiplicative site-based recessive models (Mult. recessive ($h = 0.25$); iMR) (B) The power of region-based rare variant association tests to detect association with the simulated causal gene region at significance threshold of $\alpha \leq 10^{-6}$. For region-based tests, we define power as the percent of simulation replicates in which the p-value of the test was less than α. The p-values for the ESM, c-Alpha were evaluated using 2×10^6 permutations. SKAT p-values were determined by the SKAT R package and represent numerical approximations to the presumed analytical p-value.

doi:10.1371/journal.pgen.1006573.g003

differences. The ESM test [36, 73] is the most powerful method tested for the AC, iMR, and GBR models (Fig 3b), with the c-Alpha test as a close second in some cases. For those models, the power of naive SKAT, linear kernel SKAT and SKAT-O, is always lower than the ESM and c-Alpha tests. This is peculiar since the c-Alpha test statistic is the same as the linear kernel SKAT test. The major difference between SKAT and ESM/c-Alpha is in the evaluation of statistical significance. SKAT uses an analytical approach to determine p-values while the ESM/c-Alpha tests use an explicit permutation approach. This implies that using permutation based p-values results in greater power. Yet, under the cMR model the linear kernel SKAT is the

most powerful, followed by c-alpha. The cMR model does not predict a significant burden of rare alleles and so the default beta weights of SKAT are not appropriate, and the linear kernel is superior. The ESM test does poorly on this model because there are not many marginally significant low-frequency markers. It is logical to think that these tests would all perform better if all variants were included. The massive heterogeneity in the performance of region-based rare variant tests across models strongly suggests that multiple methods should be used when prior knowledge of underlying parameters is not available. In agreement with [22, 74], we predict that population growth reduces the power to associate variants in a causal gene region with disease status (Fig 3) when the disease also impacts evolutionary fitness. We have recently released software to apply the ESM test to case control data [73] in order to facilitate applying this test to real data.

The distribution of minor allele frequencies of GWAS hits

It was noted by [4, 26], that an excess of rare significant hits, relative to empirical data, is predicted by AC models where large effect mutations contribute directly to fitness and the disease trait. We confirm that AC models are inconsistent with the empirical data (Fig 4), except when $\lambda \leq 0.01$. The empirical data in Fig 4 represent a pooled data set with the same diseases and quality filters as in [26], but updated to include more recent data. The data are described in S1 Table, and can be visualized alone more clearly in S16 Fig. Close to half of the data comes from GWAS studies uploaded to the NHGRI database after 2011, yet the same qualitative pattern is observed. This contradicts the hypothesis that the initial observation of an excess of common significant hits relative to the prediction under an AC model was simply due to small sample sizes and low marker density in early GWAS previously analyzed in [4, 26]. Yet the initial observation is in fact robust and the meta-pattern provides an appropriate point of comparison when considering the compatibility of explicit population-genetic models with existing GWAS data.

The GBR model predicts few rare significant hits and an approximately uniform distribution across the remainder of MAF domain (Fig 4), even for intermediate and large values of λ. For smaller values of λ, the GBR predicts an excess of common significant hits. The more uniform distribution of significant single markers seen under the GBR is consistent with the flatter distribution of genetic variance (Fig 1). If one considers trying to determine an approximate dominance coefficient in the GBR model, it would be found that there is a distribution of coefficients across sites. Yet, when simulating iMR model, we find that an intermediate degree of dominance, $h = 0.25$, results in distribution of significant hits which is similar to the GBR results (Fig 4).

Most of the models fail a KS test comparing the simulated and empirical distribution of significant hits(S21 Fig).The cMR ($h = 0$) model shows a visual excess of intermediate frequency variants(Fig 4), but this does not result in rejection under the KS test (S21 Fig) which is largely insensitive to deviations in the tails. According to the KS test, the remaining models(AC, GBR, iMR) perform best when there are fewer data points in the simulated data due to low GWAS power. This suggests that all models would be rejected with enough replicates. We note that there is no compelling reason to expect any specific value of λ to be a particularly good fit to the empirical data. The empirical data are composed of genome-wide data for multiple traits. We feel that the mutational parameters, λ and mutation rate to causal variants, are likely to vary across the genome and across traits. Thus, the empirical data reflect a mixture of different underlying models and ascertainment schemes. The reason we emphasize this feature of the data is to demonstrate that models with rare alleles of large effect do not necessarily imply a visual excess of rare significant GWAS hits.

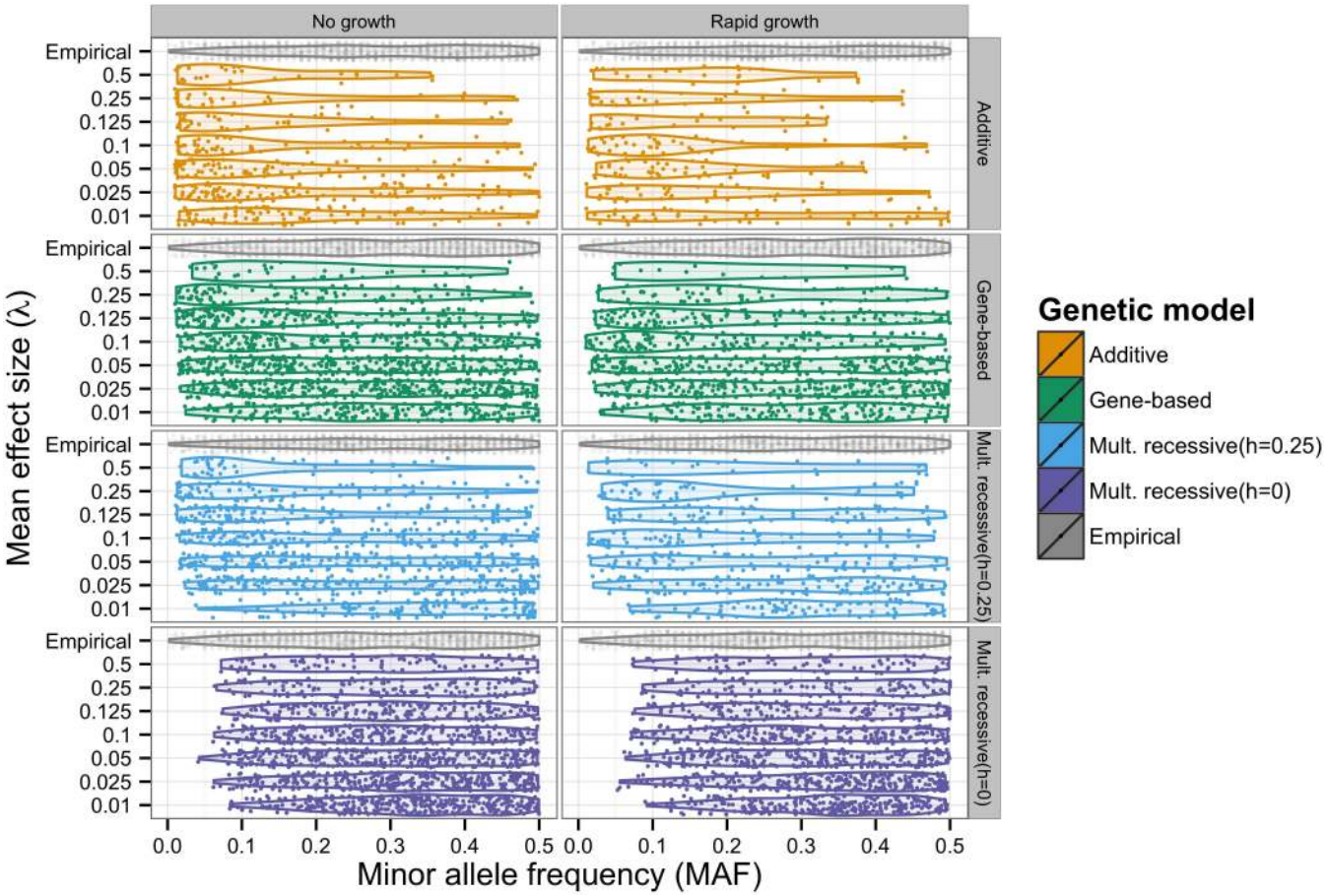

Fig 4. Distribution of significant GWAS hits. Horizontal violin plots depict the distribution of minor allele frequencies (MAF) of the most strongly associated single marker in a GWAS. Individual hits are plotted as translucent points and jittered to provide a sense of the total number and density of hits. Each panel contains simulated data pooled across model replicates for each value of λ with empirical data for comparison. Empirical data are described in Materials and Methods. In cases where more than one marker was tied for the lowest p-value, one was chosen at random. Shown here are the additive co-dominant (AC), gene-based (GBR), incomplete multiplicative recessive (Mult. recessive ($h = 0.25$); iMR) and complete multiplicative recessive (Mult. recessive ($h = 0$);cMR) models. All data shown are for models where $H^2 \sim 0.08$, because single marker test power was too low under $H^2 \sim 0.04$ to make informative density plots. To further increase the number simulated data points, we perfromed n = 1,250 replicates at each level for this figure. Simulated data were subjected to ascertainment sampling such that the MAF distribution of all markers on the simulated genotyping chip was uniform. Specific information regarding the empirical data can be obtained in S1 Table.

doi:10.1371/journal.pgen.1006573.g004

In consideration of the rare allele of large effect hypothesis, [62] proposed a model where multiple rare alleles dominate disease risk and create synthetic associations with common SNPs. However, later it was shown that this particular model was inconsistent with GWAS theoretically and empirically [4, 26, 75]. Here, we have shown that there exist models in which rare alleles explain a substantial portion of heritability that are not inconsistent with findings from GWAS. We find that the MAF distribution of significant hits in a GWAS varies widely with choice of genetic model. In particular, we confirm the results of Wray et al. [26], that AC evolutionary models predict an excess of low frequency significant hits unless trait effect sizes are quite small. Also, the cMR model predicts an excess of intermediate and common significant hits. Utilizing a GBR model or an iMR model with $h = 0.25–0.5$, reconciles this inconsistency by simultaneously predicting the importance of rare alleles of large effect and the correct allele frequency distribution among statistically significant single markers.

Conclusion

Several empirical observations provide support for the presence of gene-based recessivity underlying variation for some complex traits in humans. The minor allele frequency distribution of significant GWAS hits is relatively flat [4, 76], which our results show is consistent with either the presence of small additive effect loci or gene-/site-based partially-recessive loci with intermediate to large effects (Fig 4). Models with loci of large additive effects predict an excess of rare significant hits. Oppositely, models with complete site-based recessivity predict an excess of common significant hits for all simulated mutation effect size distributions.

SNP based estimates of dominance heritability are much lower than estimates of dominance from twins [27, 68]. Of the models we explored, only the gene-based recessive model with intermediate to large effects is consistent with the difference between twin and SNP based estimates of dominance variance (Fig 2). Under a site-based recessive model of partial recessivity (*e.g.* h = 0.25), there should be no significant difference between estimates of dominance variance from SNP and twin studies, provided that the statistical assumptions are met for both approaches (Fig 2). These results are complementary to the work by Zuk et. al [24], who show that twin studies can over estimate heritability under a model with gene interactions. It now appears clear that the underlying genetic model does not have the same impact on SNP-based and family based study designs; an issue which should be further explored. Our findings also support a more thorough investigation into the importance of compound heterozygosity in the genetics of complex traits. However, it may be difficult to directly observe non-additive gene-level effects through analysis of individual SNP markers.

Additionally, the genetic model appears to be important in the design and analysis of association studies. While changes in population size do affect the relationship between effect size and mutation frequency [48–61] (Fig 1 and S5 Fig), different mappings of genotype to trait value do this in radically different ways for the same demographic history (Fig 1). From an empirical perspective, our findings suggest that re-sequencing in large samples is likely the best way forward in the face of the allelic heterogeneity imposed by the presence of rare alleles of large effect. Resequencing of candidate genes [77–80] and exomes [40, 81–86] in case-control panels have observed an abundance of rare variants associated with case status. Here we show that under a model of mutation-selection balance on the genic level, neither current single-marker nor popular multi-marker tests are especially powerful at detecting large genomic regions harboring multiple risk variants (Fig 3). However, we show that using permutations to derive p-values improves the power of SKAT [69] with a linear kernel (equivalent test statistic to c-Alpha [38]). Similarly, another permutation based test, the ESM test [73], has more robust power across demographic and genetic models (Fig 3).

Conceptually, *cis*-effects arise naturally from the original definition of a gene in which mutant recessive alleles fail to complement [35]. We show that *cis*-effects within a locus, represented by the GBR model, can have an important impact on the population level architecture of a complex trait. This conclusion is important for future simulation studies as well as the interpretation of empirical data. It is important to note that despite our use of the term "gene-based" this model may apply to any functional genomic element in which there are multiple mutable sites affecting a trait in *cis*, not just to genes. From a theoretical perspective, our work motivates the development of a more generalized gene-based model to include arbitrary dominance and arbitrary locus size. Empirically, we find that the GBR model is broadly consistent with a variety of observations from the human statistical genetics literature. Thus, there is an evident need for improved region-based association tests and the development of genetic variance component methods for haplotypes.

Materials and Methods

Forward simulation

Using the fwdpp template library v0.2.8 [87], we implemented a forward in time individual-based simulation of a Wright-Fisher population with mutation under the infinitely many sites model [88], recombination, and selection occurring each generation. We simulated populations of size $N = 2e4$ individuals for a time of $8N$ generations with a neutral mutation rate of $\mu = 0.00125$ per gamete per generation and a per diploid per generation recombination rate of $r = 0.00125$. Deleterious mutations occurred at a rate of $\mu_d = 0.1\mu$ per gamete per generation. These parameters correspond to $\theta = 4N\mu = \rho = 4Nr = 100$ and thus our simulation approximates a 100Kb region of the human genome. For simulations with growth, we simulated an additional 500 generations of exponential growth from $N_i = 2e4$ to $N_{final} = 1e6$. This demographic model is much simpler than current models fit to empirical data [58]. However, this simple model allows us to more easily get a sense of the impact of population expansion [21, 22]. 250 simulation trials were performed for each parameter/model combination unless specified otherwise.

Exploring the gene regions contribution to heritability

Broad-sense heritability can be calculated directly from our simulated data as $H^2 = \frac{V_G}{V_P}$. We explored broad-sense heritability as a function of mean causative effect size λ under each model; $\lambda \in \{0.01, 0.025, 0.05, 0.1, 0.125, 0.25, 0.5\}$. We compare our simulation results to $V_G \sim 4\mu_d\sigma_s^2$ for additive models and $V_G \sim 2\mu_d\sigma_s^2$ for recessive models [71, 89]. In our simulations, $\sigma_s^2 = 1$, and we tuned the environmental standard deviation σ_e to generate simulations for which $E[H^2] \sim 0.04$ or ~ 0.08. For $E[H^2] \sim 0.04$, we set $\sigma_e = 0.11$ for the additive codominant model, $\sigma_e = 0.075$ for the gene based and complete multiplicative recessive models and $\sigma_e = 0.098$ for the incomplete mutliplicative recessive model ($h = 0.25$). For $E[H^2] \sim 0.08$, we set $\sigma_e = 0.075$ for the additive codominant model, $\sigma_e = 0.053$ for the gene based and complete multiplicative recessive models and $\sigma_e = 0.068$ for the incomplete mutliplicative recessive model ($h = 0.25$).

Determining the genetic load of the population

Genetic load is defined as the relative deviation in a populations fitness from the fitness optimum, $L = (w_{max} - \bar{w})/(w_{max})$. We set the phenotypic optimum to be zero; $P_{opt} = 0$. When determining fitness for the site based models, we subtract one from all phenotypes. This implies that $w_{max} = e^{-\frac{P_{opt}^2}{2\sigma_s^2}} = 1$ and that load is a simple function of the phenotypes of the population, $L = 1 - e^{-\frac{P^2}{2\sigma_s^2}}$. We also used the mean number of mutations per individual, and the mean frequency and effect sizes of segregating risk variants as proxies for the genetic load [21, 90]. Lastly, we calculated Burden Ratios (B_r) [91] as the ratio of load between an equilibrium and non-equilibrium population. We calculated B_r using both the true load and the number of mutations per individual.

Additive and dominance genetic variance over allele frequency

We used an approach based on sequential (type-1) regression sums of squares to estimate the contribution of the additive and dominance effects of variants to the total genetic variation due to a locus. Given a genotype matrix (rows are individuals and columns are risk variants) of (0,1, or 2) copies of a risk allele (*e.g.* all mutations affecting phenotype), we sort the columns by

decreasing risk mutation frequency. Then, within frequency classes, columns were sorted by decreasing effect sizes. For each variant a dominance component was also coded as 0, 2q, or 4q-2 according to the orthogonal model of [27], where q is the frequency of the variant in the population. We then used the `R` package `biglm`[92] to regress the individual genetic values (G in the previous section) onto this matrix. The variance explained by the additive and dominance effects of the m markers with $q \leq x$ is then approximately $r^2 = (\sum_{i=1}^{m} \Sigma SS_{reg,i})/(SS_{tot})$. Averaging results across replicates, this procedure results in a Monte-Carlo estimate of the fraction of V_G that is due to additive and dominance effects of variants with population frequency less than or equal to x is $(V_{A;q \leq x} + V_{D;q \leq x})/(V_{G;q \leq 1})$ [21]. This fraction can be easily partitioned into strictly additive and dominance components.

Additive and dominance heritability in random population samples

We employed three different SNP-based approaches to estimating heritability from population samples: GREMLd, minor allele frequency stratified GREMLd (MS-GREMLd)[27], and MS-Haseman-Elston (HE) regression [93, 94]. For comparison, we calculated the true total heritability in the sample as $H^2_{sample} = (V_{G;sample})/(V_{P;sample})$. Unfortunately, due to the nature of our simulated data MS-GREMLd did not result in sufficiently reliable results. Under MS-GREMLd, many replicates resulted in numerical errors in GCTA. These problems were present at a rate of less than 1/100 replicates using non-MS GREMLd, but were increased by splitting the data into multiple GRMs.

Using raw individual phenotypic values as quantitative trait values, random samples from simulated populations (n = 6000) were converted to .bed format using PLINK 1.90a [95]. PLINK was also used to test for HWE ($p < 1e{-}6$) and filter on minor allele frequency. GCTA 1.24.4 [34] was used to make genetic relatedness matrices (GRM) for both additive and dominance components with the flags –autosome and –make-grm(-d).

For non-MS runs, we tested the effect of filtering on MAF by performing the analysis on unfiltered datasets and with markers with $MAF < 0.01$ removed. For MS estimates we stratified the additive and dominance GRM's into two bins $MAF \leq 0.01$ and $MAF > 0.01$. GREMLd analysis was performed in GCTA with Fisher scoring, no variance component constraint and a max of 200 iterations. MS-HE regression was carried out by regressing the off diagonal elements of each GRM onto the cross product of the scaled and centered phenotypes in a multiple linear regression setting in R [96].

Twin studies

To simulate twin studies we sampled 2000 monozygotic (MZ) and 2000 dizygotic (DZ) twins pairs from the final generation of the simulations. Parents were sampled randomly without replacement. MZ twin pairs were formed by sampling a single gamete pair, one recombinant from each parent, and two environmental random deviates. DZ twin pairs were formed by sampling two gamete pairs, two recombinant gametes from each parent, and two environmental random deviates. Our simulated studies are ideal in that there are no correlated environmental effects, but potentially problematic due to low total heritability. We explored the use of structural equation modeling (SEM) using the package OpenMx [97], but chose to rely strictly on estimates of twin correlation obtained directly from the data. For monozygotic (MZ) twins, we used only a single child gamete pair with two unique environmental deviates. For dizygotic (DZ) twins we used two child gamete pairs, each with a unique environmental deviate. Broad sense heritability is the correlation between MZ twin pairs; $H^2 = r_{MZ}$. Under a purely additive model, the DZ twin correlation should be half of the MZ twin correlation. Non-additive genetic components of phenotypic variance reduce the DZ twin correlation. If all non-additive

heritability is due to dominance, then the dominance heritability can be calculated as twice the difference between the MZ twin correlation and two-times the DZ twin correlation: $\delta^2 = 2^*(r_{MZ} - 2^* r_{DZ})$. The additive heritability can then be calculated as the difference between the broad-sense and non-additive component: $h^2 = H^2 - \delta^2 = 4^* r_{DZ} - r_{MZ}$[29].

These direct estimates of MZ and DZ twin correlations in our simulations are reliable as we have no measurement error, shared environmental effects, gene-by-environment effects, or gene-by-gene interactions. Additionally, we only simulate a single genomic region contributing $H^2 \sim 0.04$, which made use of SEM difficult numerically. This creates a limitation in that we can not discuss when a model with dominance is a better fit to the data than the additive only model. But, the benefit of using direct estimates is that we can clearly see what signals are present in the data. To further clarify the data visualization, we pooled our 512 twin-study replicates into groups of 8, creating 64 sets of MZ-DZ twin phenotypes. This did not have an effect on the central tendencies of our estimates, but it reduced the variance. The twin study error bars in Fig 2 are based on 64 sets of 64,000 individuals, which is larger than a typical twin study. However, one reason our results have high variance is because we only simulate a single locus, rather than a whole trait.

Case-control studies

Following [36], we sampled 3000 cases and 3000 controls from each simulated population. Cases were randomly sampled from the upper 15% of phenotypic values in the population, and controls were randomly sampled from within 0.5 standard deviations of the population mean(as in [36]). This is the liability scale model (see [29]). We define a "GWAS" to be a study including all markers with MAF $\geq$5% and a re-sequencing study to include all markers. In all cases we used a minor allele count logistic regression as the single marker test. For single marker tests, the p-value cut off for significance is $p \leq 1e-08$ which is common in current GWAS [62, 98]. Power is determined by the percentage of simulation replicates in which at least one marker reaches genome wide significance.

Region-based tests of association due to rare alleles

We applied multiple region-based tests to our simulated data, ESM_K[36], several variations of SKAT [39] and c-Alpha [38]. We used the R package from the SKAT authors to implement their test (http://cran.r-project.org/web/packages/SKAT/index.html). The remaining tests were implemented in a custom R package (see SOFTWARE AVAILABILITY below). For the ESM_K and c-Alpha we performed up to 2*e*6 permutations of case-control labels to determine empirical p-values. Common variants ($q \geq 0.05$) were removed prior to performing region-based rare variant association tests.

Distribution of significant GWAS hits

Following [4, 26], we calculated the distribution of the minor allele frequency (MAF) of the most significant SNPs in a GWAS in empirical and simulated data. The empirical data was obtained from the NHGRI-EBI GWAS database (http://www.ebi.ac.uk/gwas/) on 02/05/2015. We considered the same diseases and applied the same filters as in Table 3 of [26]. Specific information regarding the empirical data can be obtained in S1 Table.

In order to mimic ascertained SNP data, we sampled markers from our case/control panels according to their minor allele frequencies [99], as done in [36]. Additionally, we removed all markers with MAF <0.01 to reflect common quality controls used in GWAS. The simulated data were grouped by genetic model, demographic scenario, heritability level, and mutation effect distribution. We then plotted the minor allele frequency of the most significant marker

with a single-marker score $-log_{10}(p) \geq 8$, for all replicates where significant markers were present.Finally, we performed a two-sample KS test in `R` between each group of simulated GWAS hit allele frequencies and the empirical data.

Human demography

We simulated a demographic model for Europeans based on [40] as described in [21]. For simplicity, we ignored migration between the European (EA) and African American (AA) populations. The model was implemented using the Python package `fwdpy` version 0.0.4, which uses `fwdpp`[87] version 0.5.1 as a C++ back-end. During the evolution of the EA population, we recorded the genetic variance in the population, V_G, and the number of deleterious mutations per diploid (a measure of genetic load [21]) every 50 generations. In a separate set of simulations, we applied the regression method described above to calculate cumulative additive genetic variance as a function of allele frequency. Because the regressions are computationally demanding, we applied the method in the generation immediately before, and at the start of, any changes in population size.

These simulations were run with no neutral mutations, and the recombination rate and mutation rate to causative mutations were the same as in the simulations described above.

The Python scripts for these simulations and iPython/Jupyter notebooks used for generating figures are available online (see Software availability section below).

Software availability

Our simulation code and code for downstream analyses are freely available at

- http://github.com/ThorntonLab/disease_sims
- http://github.com/molpopgen/buRden
- http://github.com/molpopgen/fwdpy
- http://github.com/molpopgen/TennessenEAonly

Supporting Information

S1 Text. Supplemental note.
(PDF)

S1 Fig. Broad sense heritability. Broad-sense heritability, $H^2 = (V_G)/(V_P)$, as a function of λ: the mean effect size of a new deleterious mutation, as calculated explicitly from our simulated populations. Data are plotted as the mean across model replicates ± the standard error of the mean. The solid black horizontal line shows the predicted H^2 under the respective house of cards approximation. The data is grouped by expected level of heritability and demographic scenario. For the additive model model, $H^2 \sim 8\%$ and $H^2 \sim 4\%$ imply environmental standard deviations of $\sigma_e = 0.075$ and $\sigma_e = 0.011$ respectively. For recessive models, $H^2 \sim 8\%$ and $H^2 \sim 4\%$ imply environmental standard deviations of $\sigma_e = 0.053$ and $\sigma_e = 0.075$ respectively. Shown are the additive co-dominant (AC), gene-based (GBR) and complete multiplicative recessive (Mult. recessive ($h = 0$); cMR) models.
(TIFF)

S2 Fig. Relative heritability under rapid population growth. The y-axis is the ratio of mean broad-sense heritability under recent rapid growth to mean broad sense heritability for a

constant-sized population, *e.g.* Mean$[H^2]_{growth}$/Mean$[H^2]_{constant}$. This ratio is plotted as a function of the mean effect size of causative mutations (λ). For co-dominant models, $H^2 \sim 8\%$ and $H^2 \sim 4\%$ imply environmental standard deviations of $\sigma_e = 0.075$ and $\sigma_e = 0.011$ respectively. For recessive models, $H^2 \sim 8\%$ and $H^2 \sim 4\%$ imply environmental standard deviations of $\sigma_e = 0.053$ and $\sigma_e = 0.075$ respectively. Shown are the additive co-dominant (AC), gene-based (GBR) and complete multiplicative recessive (Mult. recessive ($h = 0$); cMR) models.
(TIFF)

S3 Fig. Mean Genetic Load. Genetic load(burden), $L = \frac{w_{opt} - \bar{w}}{w_{opt}}$, as a function of λ: the mean effect size of a new deleterious mutation. Data are plotted as the mean across model replicates ± the standard error of the mean. Solid curves show values for constant sized population simulations and dashed curves show values for rapid population expansion simulations. The data is grouped by expected level of heritability and genetic model. For the additive model, $H^2 \sim 8\%$ and $H^2 \sim 4\%$ imply environmental standard deviations of $\sigma_e = 0.075$ and $\sigma_e = 0.011$ respectively. For recessive models, $H^2 \sim 8\%$ and $H^2 \sim 4\%$ imply environmental standard deviations of $\sigma_e = 0.053$ and $\sigma_e = 0.075$ respectively. Note the scales of y-axis for each plot. Shown are the additive co-dominant (AC), gene-based (GBR) and complete multiplicative recessive (Mult. recessive ($h = 0$); cMR) models.
(TIFF)

S4 Fig. Variance explained by additive and dominance effects at various frequencies. The percent of cumulative genetic variance explained by additive and dominance effects of variants with frequency less than or equal to a series of frequency values over λ. Shown here are the gene-based (GBR), additive co-dominant (AC), incomplete multiplicative recessive (Mult. recessive ($h = 0.25$); iMR) and complete multiplicative recessive (Mult. recessive ($h = 0$);cMR) models. Solid lines show the additive variance alone and dotted lines show the combined additive and dominance variance. All data shown are for models where $H^2 \sim 0.08$. These particular results are robust to changes H^2 when V_G is not changed, as is the case here. The additive and dominance genetic variance is estimated by the adjusted r^2 of the regression of all markers (and their corresponding dominance encoding) with $MAF \leq x$ onto total genotypic value (see methods for details); data are displayed as the mean of 250 simulation replicates. For each frequency level we calculated the r^2 of a linear regression of genotypes of markers with frequency below that level on to total genetic value and plot it against λ: the mean effects size of a new deleterious mutation. The data are displayed as a mean across model replicates.
(TIFF)

S5 Fig. Frequency and effect sizes of risk variants. A) The mean frequency and B) mean effect size of a segregating risk variant over λ. Note they log10 y-axis scale in A. The mean effect size is the value pulled from the exponential distribution with mean λ, not the fitness effect or the quantitative genetic effect size. The data are calculated for all risk mutations segregating in the simulated populations. Data are plotted as the mean across model replicates. For visual clarity, standard errors are not shown. In panel A, the standard error bars overlap zero under rapid population growth. The data for mean frequency are grouped by demographic scenario; the left panel shows values for constant sized population, the right panel shows values for the rapidly expanded populations. For mean effect size plots the solid curves show the constant sized population data and the dashed curves show the data for the rapidly expanded populations. Shown are the additive co-dominant (AC), gene-based (GBR) and complete multiplicative recessive (Mult. recessive ($h = 0$); cMR) models.
(TIFF)

S6 Fig. Average properties of haplotypes. A) The mean number of deleterious mutations per gamete in the population as a function of λ: the mean effect size of new causative mutation. The data plotted as mean over simulation replicates ±*se*. The data are calculated for the entire simulated population. B) The mean genetic value of a gamete, i.e. the average sum of mutational effect sizes on a gamete as a function of λ. Data are plotted as the mean across model replicates ± the standard error of the mean. In the case the gene-based recessive model, this value is also the expected value of the mean phenotype and is accurate within the sampling variance of the mean environmental variate and random pairing of gametes in diploid. Shown are the additive co-dominant (AC), gene-based (GBR) and complete multiplicative recessive (Mult. recessive ($h = 0$); cMR) models.
(TIFF)

S7 Fig. Site frequency spectrum of risk variants. For a sample $n = 100$ individuals, the relative site frequency spectrum is calculated as the proportion (y-axis) of all polymorphic sites which belong to each frequency class (x-axis). Sites with frequency was above 18 were grouped, into one category to improve visualization. The data are grouped by λ, the mean effect size of a new risk mutation, and the demographic scenario. Data shown are for simulations in which the predicted broad sense heritability is $H^2 \sim 8\%$. Plotted values are the mean proportion across simulation replicates. Shown are the additive co-dominant (AC), gene-based (GBR) and complete multiplicative recessive (Mult. recessive ($h = 0$); cMR) models.
(TIFF)

S8 Fig. Site frequency spectrum of neutral variants. For a sample $n = 100$ individuals, the relative site frequency spectrum is calculated as the proportion (y-axis) of all polymorphic sites which belong to each frequency class (x-axis). Sites with frequency was above 18 were grouped into one category to improve visualization. The data are grouped by λ, the mean effect size of a new risk mutation, and the demographic scenario. Data shown are for simulations in which the predicted broad sense heritability is $H^2 \sim 8\%$. Plotted values are the mean proportion across simulation replicates. Shown are the additive co-dominant (AC), gene-based (GBR) and complete multiplicative recessive (Mult. recessive ($h = 0$); cMR) models.
(TIFF)

S9 Fig. Site frequency spectrum of risk and neutral variants. For a sample $n = 100$ individuals, the relative site frequency spectrum is calculated as the proportion (y-axis) of all polymorphic sites which belong to each frequency class (x-axis). Neutral variants are in orange and risk variants are shown in green. Y-axis is on a square-root scale and X-axis is on a log10 scale to improve visualization. The data are grouped by λ, the mean effect size of a new risk mutation, the demographic scenario and genetic model. Data shown are for simulations in which the predicted broad sense heritability is $H^2 \sim 8\%$. Plotted values are the mean proportion across simulation replicates. Shown are the additive co-dominant (AC), gene-based (GBR) and complete multiplicative recessive (Mult. recessive ($h = 0$); cMR) models.
(TIFF)

S10 Fig. Distribution of significant hits under site based recessive models with incomplete dominance. Horizontal violin plots depict the distribution of minor allele frequencies (MAF) of the most strongly associated single marker in a GWAS. Individual hits are plotted as translucent points and jittered to provide a sense of the total number and density of hits. Each panel contains simulated data pooled across model replicates for each value of λ, with empirical data for comparison. The degree of dominance h was varied from 0.1 to 0.75; perfect co-dominance here is h = 1. Empirical data were downloaded from the NHGRI-EBI GWAS database (http://www.ebi.ac.uk/gwas/) on 02/03/2015, diseases and inclusion criteria are as in [26]. In cases

where more than one marker was tied for the lowest p-value, one was chosen at random. Simulated data were subjected to ascertainment sampling such that the MAF distribution of all markers on the simulated genotyping chip was uniform. Specific information regarding the empirical data can be obtained in S1 Table.
(TIFF)

S11 Fig. Skew of gamete properties. The skewness A) the number of mutations per gamete and B) the genetic value (sum of mutational effects) of a gamete over λ. The data are calculated for all risk mutations segregating in the simulated populations. Moments were calculated using the boost C++ statistical accumulators library. Data are plotted as the mean across model replicates ± the standard error of the mean. Shown are the additive co-dominant (AC), gene-based (GBR) and complete multiplicative recessive (Mult. recessive ($h = 0$); cMR) models.
(TIFF)

S12 Fig. Kurtosis of gamete properties. The kurtosis A) the number of mutations per gamete and B) the genetic value (sum of mutational effects) of a gamete over λ. The data are calculated for all risk mutations segregating in the simulated populations. Moments were calculated using the boost C++ statistical accumulators library. Data are plotted as the mean across model replicates ± the standard error of the mean. Shown are the additive co-dominant (AC), gene-based (GBR) and complete multiplicative recessive (Mult. recessive ($h = 0$); cMR) models.
(TIFF)

S13 Fig. Properties of Sample Heritability. Broad-sense heritability in a population sample of 6000 as a proportion of population wide broad-sense heritability. Data are grouped by demographic scenario, model and λ. The arbitrary dominance coefficient is parameterized such that $h = 0$ is complete recessivity, $h = 1$ would be exact co-dominance and $h = 2$ would be complete dominance. Multiplicative recessive (MR) models shown are only for $h = 0.25$.
(TIFF)

S14 Fig. Regression Based Estimates of Genetic Variance. (A) Regression estimates of variance explained by markers versus the classical formula $2pq\alpha^2$. (B) Cumulative percent of variance explained across the risk allele frequency, based on regression estimates and classical formula. 1000 unlinked markers were simulated with effects drawn from an exponential distribution with mean 0.1 and population frequencies drawn from the neutral Wright-Fisher allele frequency distribution. Sample data for 5000 individuals were then generated by sampling genotypes at each marker based on its allele frequency. We plot the regression estimate of variance explained by each marker against Fisher's classic result [9]: $V_G = 2pq\alpha^2$.
(TIFF)

S15 Fig. Dominance for fitness effects versus dominance for trait effects. The dominance of fitness effects, $\frac{s_{het}}{s_{hom}}$, as a function of the dominance for trait effects, h. Values are based on idealized fitness effects of a mutation on a previously unaffected genetic background. The the relationship between fitness and trait dominance is influenced by the trait effect size. We varied trait effect sizes from 0.01 to 1, and values are colored based on the trait effect.
(TIFF)

S16 Fig. Empirical distribution of GWAS hits. Histogram GWAS hits (n = 1208) obtained from the NHGRI-EBI GWAS database for disease discussed in [26]. Data are described in S1 Table.
(TIFF)

S17 Fig. Additive genetic variance explained over allele frequency under the Tennessen et al. [40] model for European demography. (A) Population size change over time. Colored numbers represent population sizes at different times where we estimated the cumulative additive genetic variance (V_A) as a function of allele frequency using regression (see Materials and Methods). These time points represent key changes in population size in this model. (B-D) Estimated cumulative V_A as a function of frequency for three different mean effect sizes ($\lambda \in 0.1,0.25,0.5$). Solid lines are the standard additive model. Dashed lines are the GBR model of [36]. For all time points, the same total percent of variance is explained, with the exception of the line labelled "bottleneck". For larger effect sizes under the GBR model, the bottleneck increases the total V_A explained by all mutations. This effect is, however, short lived, and disappears by the end of the epoch defined by $N = 1{,}861$. This result is consistent with transient increases in variation under recessive models reported by [21].
(TIFF)

S18 Fig. Genetic variance and load over time under the Tennessen *et al.*[40] model for European demography. The left column of panels shows how V_G changes over time under this model. The right column shows how the mean number of deleterious mutations per individual changes. The models shown are: a = additive, g = GBR, and m = multiplicative with varying degrees of dominance (h). The main difference is between additive models (a or m with $h = 1.0$) and recessive models (g or m with small h). The former models are largely insensitive to changes in N, while the recessive models show transient increases in V_G and "load" immediately following a bottleneck (consistent with [21]). However, at the final time point representing the "modern European population", all mean V_G is $\approx 4\mu$ for additive models and $\approx 2\mu$ for recessive models [71, 89], and recessive models show larger loads as expected [21].
(TIFF)

S19 Fig. The burden ratio over time. The burden ratio [91] is calculated as the ratio of genetic load between simulations with only ancient growth and those with an additional recent bottleneck and growth. Here load is calculated as the average deviation from optimum fitness due to (left) fixed mutations, (middle) segregating mutations and (right) all mutations. Because of the use of the Gaussian fitness function, the total load is not the sum of the fixed and segregating load. The models shown are: a = additive, g = GBR, and m = multiplicative with varying degrees of dominance (h). For large effect size models, under which there are relatively more mutations that experience strong selection, we see the characteristic drop in the burden ratio following the bottleneck and rebound following re-expansion [91].
(TIFF)

S20 Fig. The burden ratio based on mutations over time. The burden ratio [91] is calculated as the ratio of genetic load between simulations with only ancient growth and those with an additional recent bottleneck and growth. Here load is calculated as the average number of (left) fixed mutations, (middle) segregating mutations and (right) all mutations. The models shown are: a = additive, g = GBR, and m = multiplicative with varying degrees of dominance (h).
(TIFF)

S21 Fig. Non-parametric comparison between empirical and simulated GWAS hits. A non-parametric comparison between distribution of allele frequencies between simulated and empirical GWAS hits. Shown are the -log10(p) values from the two-sample Kolmogorov-Smirnov test between the simulated and empirical allele frequencies. The lower and upper horizontal lines show where p = 0.05 and p = 0.001 respectively. Empirical data were downloaded from the NHGRI-EBI GWAS database (http://www.ebi.ac.uk/gwas/) on 02/03/2015, diseases

and inclusion criteria are as in [26]. In cases where more than one marker was tied for the lowest p-value, one was chosen at random. Simulated data were subjected to ascertainment sampling such that the MAF distribution of all markers on the simulated genotyping chip was uniform. Specific information regarding the empirical data can be obtained in S1 Table.
(TIFF)

S22 Fig. The cumulative distribution of 2*Ns*. The probability of a new mutation with $2Ns \leq x$ on a log scale for various values of λ. The dashed lines show the analytical result and the solid curves are empirical cumulative distribution functions based on a sample of 500 mutation effects from an exponential distribution. The analytical result is an approximation obtained by assuming there is only a single deleterious mutation.
(TIFF)

S23 Fig. The probability density function of *s*. The probability of a new mutation with $s = x$ on a log scale for various values of λ. The analytical result is an approximation obtained by assuming there is only a single deleterious mutation. For λ of 0.25 and 0.5 there is a large mass of lethals near $s = 1$.
(TIFF)

S1 Table. Details of Empirical GWAS Data. This table contains information specifying the empirical studies used in the manuscript. The data were obtained from the NHGRI-EBI catalog of published genome-wide association studies. All information fields contained in the download of the GWAS catalog are presented here.
(XLSX)

Acknowledgments

We are thankful to Joseph Farran, Harry Mangalam, Adam Brenner, Garr Updegraff, and Edward Xia for administering the University of California, Irvine High Performance Computing cluster. We are thankful to Kirk Lohmueller for helpful detailed comments throughout this project. We would like to thank Peter Andolfatto, Bogdan Pasaniuc and Nick Mancuso for helpful discussion.

Author Contributions

Conceptualization: JSS ADL KRT.

Data curation: JSS.

Formal analysis: JSS KRT.

Funding acquisition: KRT.

Investigation: JSS KRT.

Methodology: JSS KRT.

Project administration: KRT.

Resources: KRT ADL.

Software: KRT JSS.

Supervision: KRT.

Validation: JSS KRT.

Visualization: JSS.

Writing – original draft: JSS.

Writing – review & editing: JSS ADL KRT.

References

1. Welter D, MacArthur J, Morales J, Burdett T, Hall P, Junkins H, et al. The NHGRI GWAS Catalog, a curated resource of SNP-trait associations. Nucleic Acids Research. 2014; 42(December 2013):1001–1006. doi: 10.1093/nar/gkt1229 PMID: 24316577
2. Manolio TA, Collins FS, Cox NJ, Goldstein DB, Hindorff LA, Hunter DJ, et al. Finding the missing heritability of complex diseases. Nature. 2009 oct; 461(7265):747–53. Available from: http://www.pubmedcentral.nih.gov/articlerender.fcgi?artid=2831613&tool=pmcentrez&rendertype=abstract. doi: 10.1038/nature08494 PMID: 19812666
3. Visscher PM, Brown MA, McCarthy MI, Yang J. Five years of GWAS discovery. American journal of human genetics. 2012 jan; 90(1):7–24. Available from: http://www.sciencedirect.com/science/article/pii/S0002929711005337. doi: 10.1016/j.ajhg.2011.11.029 PMID: 22243964
4. Gibson G. Rare and common variants: twenty arguments. Nature Reviews Genetics. 2012; 13(2):135–145. Available from: http://dx.doi.org/10.1038/nrg3118. PMID: 22251874
5. Robinson MR, Wray NR, Visscher PM. Explaining additional genetic variation in complex traits. Trends in Genetics. 2014; 30:124–132. Available from: http://dx.doi.org/10.1016/j.tig.2014.02.003. PMID: 24629526
6. Eichler EE, Flint J, Gibson G, Kong A, Leal SM, Moore JH, et al. Missing heritability and strategies for finding the underlying causes of complex disease. Nature reviews Genetics. 2010 jun; 11(6):446–50. Available from: http://dx.doi.org/10.1038/nrg2809. PMID: 20479774
7. Wei WH, Hemani G, Haley CS. Detecting epistasis in human complex traits. Nature Reviews Genetics. 2014; 15(11):722–733. Available from: http://dx.doi.org/10.1038/nrg3747. PMID: 25200660
8. Zuk O, Hechter E, Sunyaev SR, Lander ES. The mystery of missing heritability: Genetic interactions create phantom heritability. Proceedings of the National Academy of Sciences. 2012; 109(4):1193–1198. doi: 10.1073/pnas.1119675109 PMID: 22223662
9. Fisher RA. The Genetical Theory Of Natural Selection: Fisher R. A: Free Download & Streaming: Internet Archive. Oxford, UK; 1930. Available from: https://archive.org/details/geneticaltheoryo031631mbp.
10. Visscher PM, Hill WG, Wray NR. Heritability in the genomics era–concepts and misconceptions. Nature reviews Genetics. 2008 apr; 9(4):255–66. Available from: http://dx.doi.org/10.1038/nrg2322. PMID: 18319743
11. McClellan J, King MC. Genetic heterogeneity in human disease. Cell. 2010 apr; 141(2):210–7. Available from: http://www.sciencedirect.com/science/article/pii/S009286741000320X. doi: 10.1016/j.cell.2010.03.032 PMID: 20403315
12. Cirulli ET, Goldstein DB. Uncovering the roles of rare variants in common disease through whole-genome sequencing. Nature reviews Genetics. 2010 jun; 11(6):415–25. Available from: http://dx.doi.org/10.1038/nrg2779. PMID: 20479773
13. Visscher PM, Goddard ME, Derks EM, Wray NR. Evidence-based psychiatric genetics, AKA the false dichotomy between common and rare variant hypotheses. Molecular psychiatry. 2012 may; 17(5):474–85. Available from: http://dx.doi.org/10.1038/mp.2011.65. PMID: 21670730
14. Yang J, Benyamin B, McEvoy BP, Gordon S, Henders AK, Nyholt DR, et al. Common SNPs explain a large proportion of the heritability for human height. Nature genetics. 2010 jul; 42(7):565–9. Available from: http://dx.doi.org/10.1038/ng.608. PMID: 20562875
15. Golan D, Lander ES, Rosset S. Measuring missing heritability: Inferring the contribution of common variants. Proceedings of the National Academy of Sciences of the United States of America. 2014.
16. Yang J, Bakshi A, Zhu Z, Hemani G, Vinkhuyzen AAE, Lee SH, et al. Genetic variance estimation with imputed variants finds negligible missing heritability for human height and body mass index. Nature Genetics. 2015 aug;advance on. Available from: http://dx.doi.org/10.1038/ng.3390. doi: 10.1038/ng.3390 PMID: 26323059
17. Pritchard JK. Are rare variants responsible for susceptibility to complex diseases? American journal of human genetics. 2001 jul; 69(1):124–37. Available from: http://www.pubmedcentral.nih.gov/articlerender.fcgi?artid=1226027&tool=pmcentrez&rendertype=abstract. doi: 10.1086/321272 PMID: 11404818

18. Eyre-Walker A. Evolution in health and medicine Sackler colloquium: Genetic architecture of a complex trait and its implications for fitness and genome-wide association studies. Proceedings of the National Academy of Sciences of the United States of America. 2010; 107 Suppl:1752–1756. doi: 10.1073/pnas.0906182107 PMID: 20133822

19. Park JH, Wacholder S, Gail MH, Peters U, Jacobs KB, Chanock SJ, et al. Estimation of effect size distribution from genome-wide association studies and implications for future discoveries. Nature genetics. 2010 jul; 42(7):570–5. Available from: http://dx.doi.org/10.1038/ng.610. PMID: 20562874

20. Agarwala V, Flannick J, Sunyaev S, Altshuler D. Evaluating empirical bounds on complex disease genetic architecture. Nature genetics. 2013; 45(12):1418–27. Available from: http://www.ncbi.nlm.nih.gov/pubmed/24141362. doi: 10.1038/ng.2804 PMID: 24141362

21. Simons YB, Turchin MC, Pritchard JK, Sella G. The deleterious mutation load is insensitive to recent population history. Nature genetics. 2014; 46(August 2013):220–4. Available from: http://www.ncbi.nlm.nih.gov/pubmed/24509481. doi: 10.1038/ng.2896 PMID: 24509481

22. Lohmueller KE. The impact of population demography and selection on the genetic architecture of complex traits. PLoS genetics. 2014 may; 10(5):e1004379. Available from: http://dx.plos.org/10.1371/journal.pgen.1004379. doi: 10.1371/journal.pgen.1004379 PMID: 24875776

23. Uricchio LH, Zaitlen NA, Ye CJ, Witte JS, Hernandez RD. Selection and explosive growth alter genetic architecture and hamper the detection of causal rare variants. Genome Research. 2016 may;Available from: http://genome.cshlp.org/lookup/doi/10.1101/gr.202440.115. doi: 10.1101/gr.202440.115 PMID: 27197206

24. Zuk O, Schaffner SF, Samocha K, Do R, Hechter E, Kathiresan S, et al. Searching for missing heritability: designing rare variant association studies. Proceedings of the National Academy of Sciences of the United States of America. 2014; 111:E455–64. Available from: http://www.pubmedcentral.nih.gov/articlerender.fcgi?artid=3910587&tool=pmcentrez&rendertype=abstract. doi: 10.1073/pnas.1322563111 PMID: 24443550

25. Caballero A, Tenesa A, Keightley PD. The Nature of Genetic Variation for Complex Traits Revealed by GWAS and Regional Heritability Mapping Analyses. Genetics. 2015 oct; 201(4):1601–13. Available from: http://genetics.org/content/201/4/1601.abstract. doi: 10.1534/genetics.115.177220 PMID: 26482794

26. Wray NR, Purcell SM, Visscher PM. Synthetic associations created by rare variants do not explain most GWAS results. PLoS Biology. 2011; 9(1). doi: 10.1371/journal.pbio.1000579 PMID: 21267061

27. Zhu Z, Bakshi A, Vinkhuyzen AE, Hemani G, Lee S, Nolte I, et al. Dominance Genetic Variation Contributes Little to the Missing Heritability for Human Complex Traits. The American Journal of Human Genetics. 2015;p. 377–385. Available from: http://linkinghub.elsevier.com/retrieve/pii/S0002929715000099. doi: 10.1016/j.ajhg.2015.01.001 PMID: 25683123

28. Chen HS, Hutter CM, Mechanic LE, Amos CI, Bafna V, Hauser ER, et al. Genetic simulation tools for post-genome wide association studies of complex diseases. Genetic epidemiology. 2015 jan; 39(1):11–9. Available from: http://www.ncbi.nlm.nih.gov/pubmed/25371374. doi: 10.1002/gepi.21870 PMID: 25371374

29. Falconer D, Mackay TFC. Introduction to Quantitative Genetics, Ed. 2. Harlow, Essex, UK: Longmans Green; 1996.

30. Risch N. Linkage strategies for genetically complex traits. III. The effect of marker polymorphism on analysis of affected relative pairs. American journal of human genetics. 1990; 46:242–253. PMID: 2301394

31. Risch N. Linkage strategies for genetically complex traits. I. Multilocus models. American journal of human genetics. 1990; 46:222–228. PMID: 2301392

32. Spencer CCA, Su Z, Donnelly P, Marchini J. Designing Genome-Wide Association Studies: Sample Size, Power, Imputation, and the Choice of Genotyping Chip. PLoS Genetics. 2009 may; 5(5):e1000477. Available from: http://journals.plos.org/plosgenetics/article?id=10.1371/journal.pgen.1000477. doi: 10.1371/journal.pgen.1000477 PMID: 19492015

33. Wellcome T, Case T, Consortium C. Genome-wide association study of 14,000 cases of seven common diseases and 3,000 shared controls. Nature. 2007; 447(June):661–678. doi: 10.1038/nature05911 PMID: 17554300

34. Yang J, Lee SH, Goddard ME, Visscher PM. GCTA: a tool for genome-wide complex trait analysis. American journal of human genetics. 2011 jan; 88(1):76–82. Available from: http://www.sciencedirect.com/science/article/pii/S0002929710005987. doi: 10.1016/j.ajhg.2010.11.011 PMID: 21167468

35. Benzer S. Fine Structure of a Genetic Region in Bacteriophage. Proceedings of the National Academy of Sciences of the United States of America. 1955 jun; 41(6):344–354. Available from: http://www.ncbi.nlm.nih.gov/pmc/articles/PMC528093/?tool=pmcentrez. doi: 10.1073/pnas.41.6.344 PMID: 16589677

36. Thornton KR, Foran AJ, Long AD. Properties and Modeling of GWAS when Complex Disease Risk Is Due to Non-Complementing, Deleterious Mutations in Genes of Large Effect. PLoS Genetics. 2013; 9 (2). doi: 10.1371/journal.pgen.1003258 PMID: 23437004

37. Strachan T and Read A. Human Molecular Genetics (New York: Garland Science, Taylor \& Francis Group). 2011.

38. Neale BM, Rivas Ma, Voight BF, Altshuler D, Devlin B, Orho-Melander M, et al. Testing for an unusual distribution of rare variants. PLoS Genetics. 2011; 7(3). doi: 10.1371/journal.pgen.1001322 PMID: 21408211

39. Wu MC, Lee S, Cai T, Li Y, Boehnke M, Lin X. Rare-variant association testing for sequencing data with the sequence kernel association test. American Journal of Human Genetics. 2011; 89(1):82–93. Available from: http://dx.doi.org/10.1016/j.ajhg.2011.05.029. PMID: 21737059

40. Tennessen Ja, Bigham aW, O'Connor TD, Fu W, Kenny EE, Gravel S, et al. Evolution and Functional Impact of Rare Coding Variation from Deep Sequencing of Human Exomes. Science. 2012; 337 (6090):64–69. doi: 10.1126/science.1219240 PMID: 22604720

41. Burger RR. The mathematical theory of selection, recombination, and mutation. Wiley; 2000.

42. Haldane JBS. The cost of natural selection; 1957.

43. Charlesworth B, Morgan MT, Charlesworth D. The effect of deleterious mutations on neutral molecular variation. Genetics. 1993; 134(4):1289–1303. Available from: http://www.genetics.org/content/134/4/1289.full.pdf+html?sid=223c0d2d-8c37-4cae-9a0d-25fe7274716fpapers2://publication/uuid/009B9585-7ABD-4806-901D-9853FD506745. PMID: 8375663

44. Risch N, Merikangas K. The future of genetic studies of complex human diseases. Science (New York, NY). 1996 sep; 273(5281):1516–7. Available from: http://www.ncbi.nlm.nih.gov/pubmed/8801636. doi: 10.1126/science.273.5281.1516 PMID: 8801636

45. Sham PC, Purcell SM. Statistical power and significance testing in large-scale genetic studies. Nature reviews Genetics. 2014 may; 15(5):335–46. Available from: http://dx.doi.org/10.1038/nrg3706. PMID: 24739678

46. Uricchio LH, Witte JS, Hernandez RD. Selection and explosive growth may hamper the performance of rare variant association tests; 2015. Available from: http://www.biorxiv.org/content/early/2015/03/01/015917.abstract. doi: 10.1101/gr.202440.115 PMID: 27197206

47. Hill WG, Goddard ME, Visscher PM. Data and theory point to mainly additive genetic variance for complex traits. PLoS genetics. 2008 feb; 4(2):e1000008. Available from: http://journals.plos.org/plosgenetics/article?id=10.1371/journal.pgen.1000008. doi: 10.1371/journal.pgen.1000008 PMID: 18454194

48. Griffiths RC, Tavaré S. Sampling theory for neutral alleles in a varying environment. Philosophical transactions of the Royal Society of London Series B, Biological sciences. 1994 jun; 344(1310):403–10. Available from: http://www.ncbi.nlm.nih.gov/pubmed/7800710. doi: 10.1098/rstb.1994.0079 PMID: 7800710

49. Griffiths RC, Tavare S. Ancestral Inference in Population Genetics. Statistical Science. 1994 aug; 9 (3):307–319. Available from: http://projecteuclid.org/euclid.ss/1177010378. doi: 10.1214/ss/1177010378

50. Rogers A, Harpending H. Population growth makes waves in the distribution of pairwise genetic differences. Mol Biol Evol. 1992 may; 9(3):552–569. Available from: http://mbe.oxfordjournals.org/content/9/3/552. PMID: 1316531

51. Fu YX. Statistical Tests of Neutrality of Mutations Against Population Growth, Hitchhiking and Background Selection. Genetics. 1997 oct; 147(2):915–925. Available from: http://www.genetics.org/content/147/2/915.short. PMID: 9335623

52. Beaumont MA. Detecting Population Expansion and Decline Using Microsatellites. Genetics. 1999 dec; 153(4):2013–2029. Available from: http://www.genetics.org/content/153/4/2013.short. PMID: 10581303

53. Aris-Brosou S, Excoffier L. The impact of population expansion and mutation rate heterogeneity on DNA sequence polymorphism. Molecular Biology and Evolution. 1996 mar; 13(3):494–504. Available from: http://mbe.oxfordjournals.org/content/13/3/494.short. PMID: 8742638

54. Coventry A, Bull-Otterson LM, Liu X, Clark AG, Maxwell TJ, Crosby J, et al. Deep resequencing reveals excess rare recent variants consistent with explosive population growth. Nature communications. 2010 jan; 1:131. Available from: http://dx.doi.org/10.1038/ncomms1130. PMID: 21119644

55. Gao F, Keinan A. High burden of private mutations due to explosive human population growth and purifying selection. BMC genomics. 2014; 15 Suppl 4(Suppl 4):S3. Available from: http://www.ncbi.nlm.nih.gov/pubmed/25056720. doi: 10.1186/1471-2164-15-S4-S3 PMID: 25056720

56. Gazave E, Chang D, Clark AG, Keinan A. Population growth inflates the per-individual number of deleterious mutations and reduces their mean effect. Genetics. 2013; 195(3):969–978. doi: 10.1534/genetics.113.153973 PMID: 23979573

57. Gazave E, Ma L, Chang D, Coventry A, Gao F, Muzny D, et al. Neutral genomic regions refine models of recent rapid human population growth. Proceedings of the National Academy of Sciences of the United States of America. 2014; 111(2):757–62. Available from: http://www.pubmedcentral.nih.gov/articlerender.fcgi?artid=3896169&tool=pmcentrez&rendertype=abstract. doi: 10.1073/pnas.1310398110 PMID: 24379384

58. Gravel S, Henn BM, Gutenkunst RN, Indap AR, Marth GT, Clark AG, et al. Demographic history and rare allele sharing among human populations. Proceedings of the National Academy of Sciences. 2011 jul; 108(29):11983–11988. Available from: http://www.pnas.org/content/108/29/11983.short. doi: 10.1073/pnas.1019276108 PMID: 21730125

59. Keinan a, Clark aG. Recent Explosive Human Population Growth Has Resulted in an Excess of Rare Genetic Variants. Science. 2012; 336(6082):740–743. doi: 10.1126/science.1217283 PMID: 22582263

60. Kimmel M, Chakraborty R, King JP, Bamshad M, Watkins WS, Jorde LB. Signatures of Population Expansion in Microsatellite Repeat Data. Genetics. 1998 apr; 148(4):1921–1930. Available from: http://www.genetics.org/content/148/4/1921.short. PMID: 9560405

61. Reich DE, Goldstein DB. Genetic evidence for a Paleolithic human population expansion in Africa. Proceedings of the National Academy of Sciences. 1998 jul; 95(14):8119–8123. Available from: http://www.pnas.org/content/95/14/8119.full. doi: 10.1073/pnas.95.14.8119 PMID: 9653150

62. Dickson SP, Wang K, Krantz I, Hakonarson H, Goldstein DB. Rare Variants Create Synthetic Genome-Wide Associations. PLoS Biology. 2010; 8(1). doi: 10.1371/journal.pbio.1000294 PMID: 20126254

63. Maher MC, Uricchio LH, Torgerson DG, Hernandez RD. Population genetics of rare variants and complex diseases. Human heredity. 2012 jan; 74(3-4):118–28. Available from: http://www.pubmedcentral.nih.gov/articlerender.fcgi?artid=3698246&tool=pmcentrez&rendertype=abstract. doi: 10.1159/000346826 PMID: 23594490

64. Reich DE, Lander ES. On the allelic spectrum of human disease. Trends in Genetics. 2001 sep; 17(9):502–510. Available from: http://www.sciencedirect.com/science/article/pii/S0168952501024106. doi: 10.1016/S0168-9525(01)02410-6 PMID: 11525833

65. Mancuso N, Rohland N, Rand KA, Tandon A, Allen A, Quinque D, et al. The contribution of rare variation to prostate cancer heritability. Nature genetics. 2015 nov;advance on. Available from: http://dx.doi.org/10.1038/ng.3446. PMID: 26569126

66. Naciri-Graven Y, Goudet J. The additive genetic variance after bottlenecks is affected by the number of loci involved in epistatic interactions. Evolution. 2003; 57(574):706–716. Available from: http://www.jstor.org/stable/3094609http://about.jstor.org/terms. doi: 10.1554/0014-3820(2003)057%5B0706:TAGVAB%5D2.0.CO;2 PMID: 12778542

67. Barton NH, Turelli M, Barton NH, Turelli M. Effects of Genetic Drift on Variance Components under a General Model of Epistasis. Evolution. 2004; 58(5810):2111–2132. Available from: http://www.jstor.org/stable/3449464http://about.jstor.org/terms. doi: 10.1554/03-684 PMID: 15562679

68. Chen X, Kuja-Halkola R, Rahman I, Arpegård J, Viktorin A, Karlsson R, et al. Dominant Genetic Variation and Missing Heritability for Human Complex Traits: Insights from Twin versus Genome-wide Common SNP Models. The American Journal of Human Genetics. 2015 nov; 97(5):708–714. Available from: http://linkinghub.elsevier.com/retrieve/pii/S0002929715004061. doi: 10.1016/j.ajhg.2015.10.004 PMID: 26544805

69. Lee E, Luo J, Su YC, Lewinger JP, Schumacher FR, Van Den Berg D, et al. Hormone metabolism pathway genes and mammographic density change after quitting estrogen and progestin combined hormone therapy in the California Teachers Study. Breast cancer research: BCR. 2014 jan; 16(6):477. Available from: http://breast-cancer-research.com/content/16/6/477. doi: 10.1186/s13058-014-0477-8 PMID: 25499601

70. Lee SH, Yang J, Chen GB, Ripke S, Stahl EA, Hultman CM, et al. Estimation of SNP heritability from dense genotype data. American journal of human genetics. 2013 dec; 93(6):1151–5. Available from: http://www.sciencedirect.com/science/article/pii/S0002929713004722. doi: 10.1016/j.ajhg.2013.10.015 PMID: 24314550

71. Turelli M. Heritable genetic variation via mutation-selection balance: Lerch's zeta meets the abdominal bristle. Theoretical Population Biology. 1984 apr; 25(2):138–193. Available from: http://www.sciencedirect.com/science/article/pii/0040580984900170. doi: 10.1016/0040-5809(84)90017-0 PMID: 6729751

72. Chapman JM, Cooper JD, Todd JA, Clayton DG. Detecting disease associations due to linkage disequilibrium using haplotype tags: a class of tests and the determinants of statistical power. Human heredity. 2003; 56(1-3):18–31. Available from: http://www.ncbi.nlm.nih.gov/pubmed/14614235. doi: 73729 PMID: 14614235

73. Sanjak JS, Long AD, Thornton KR. Efficient Software for Multi-marker, Region-Based Analysis of GWAS Data. G3 (Bethesda, Md). 2016 feb;Available from: http://www.ncbi.nlm.nih.gov/pubmed/26865700. doi: 10.1534/g3.115.026013 PMID: 26865700

74. Uricchio LH, Torres R, Witte JS, Hernandez RD. Population genetic simulations of complex phenotypes with implications for rare variant association tests. Genetic epidemiology. 2015 jan; 39(1):35–44. Available from: http://www.ncbi.nlm.nih.gov/pubmed/25417809. doi: 10.1002/gepi.21866 PMID: 25417809

75. Orozco G, Barrett JC, Zeggini E. Synthetic associations in the context of genome-wide association scan signals. Human molecular genetics. 2010 oct; 19(R2):R137–44. Available from: http://hmg.oxfordjournals.org/content/19/R2/R137.long. doi: 10.1093/hmg/ddq368 PMID: 20805105

76. Wray NR, Purcell SM, Visscher PM. Synthetic associations created by rare variants do not explain most GWAS results. PLoS biology. 2011; 9(1):e1000579. Available from: http://www.ncbi.nlm.nih.gov/pubmed/21267061http://www.pubmedcentral.nih.gov/articlerender.fcgi?artid=PMC3022526. doi: 10.1371/journal.pbio.1000579 PMID: 21267061

77. Johansen CT, Wang J, Lanktree MB, Cao H, McIntyre AD, Ban MR, et al. Excess of rare variants in genes identified by genome-wide association study of hypertriglyceridemia. Nature genetics. 2010 aug; 42(8):684–7. Available from: http://www.pubmedcentral.nih.gov/articlerender.fcgi?artid=3017369&tool=pmcentrez&rendertype=abstract. doi: 10.1038/ng.628 PMID: 20657596

78. Kotowski IK, Pertsemlidis A, Luke A, Cooper RS, Vega GL, Cohen JC, et al. A spectrum of PCSK9 alleles contributes to plasma levels of low-density lipoprotein cholesterol. American journal of human genetics. 2006; 78(3):410–422. doi: 10.1086/500615 PMID: 16465619

79. Marini NJ, Gin J, Ziegle J, Keho KH, Ginzinger D, Gilbert Da, et al. The prevalence of folate-remedial MTHFR enzyme variants in humans. Proceedings of the National Academy of Sciences of the United States of America. 2008; 105(23):8055–8060. doi: 10.1073/pnas.0802813105 PMID: 18523009

80. Romeo S, Pennacchio LA, Fu Y, Boerwinkle E, Tybjaerg-Hansen A, Hobbs HH, et al. Population-based resequencing of ANGPTL4 uncovers variations that reduce triglycerides and increase HDL. Nature genetics. 2007 apr; 39(4):513–6. Available from: http://www.pubmedcentral.nih.gov/articlerender.fcgi?artid=2762948&tool=pmcentrez&rendertype=abstract. doi: 10.1038/ng1984 PMID: 17322881

81. Huyghe JR, Jackson AU, Fogarty MP, Buchkovich ML, Stančáková A, Stringham HM, et al. Exome array analysis identifies new loci and low-frequency variants influencing insulin processing and secretion. Nature genetics. 2013; 45(2):197–201. Available from: http://dx.doi.org/10.1038/ng.2507. PMID: 23263489

82. Wessel J, Goodarzi MO. Low-frequency and rare exome chip variants associate with fasting glucose and type 2 diabetes susceptibility. Nature Communications. 2015; 6:5897. Available from: http://www.nature.com/doifinder/10.1038/ncomms6897. doi: 10.1038/ncomms6897 PMID: 25631608

83. Purcell SM, Moran JL, Fromer M, Ruderfer D, Solovieff N, Roussos P, et al. A polygenic burden of rare disruptive mutations in schizophrenia. Nature. 2014; 506(7487):185–90. Available from: http://www.ncbi.nlm.nih.gov/pubmed/24463508. doi: 10.1038/nature12975 PMID: 24463508

84. Nelson MR, Wegmann D, Ehm MG, Kessner D, St Jean P, Verzilli C, et al. An abundance of rare functional variants in 202 drug target genes sequenced in 14,002 people. Science (New York, NY). 2012 jul; 337(6090):100–4. Available from: http://www.sciencemag.org/content/337/6090/100.abstract. doi: 10.1126/science.1217876 PMID: 22604722

85. Luciano M, Svinti V, Campbell A, Marioni RE, Hayward C, Wright AF, et al. Exome Sequencing to Detect Rare Variants Associated With General Cognitive Ability: A Pilot Study. Twin research and human genetics: the official journal of the International Society for Twin Studies. 2015 mar;p. 1–9. Available from: http://journals.cambridge.org/abstract_S1832427415000109. doi: 10.1017/thg.2015.10 PMID: 25744449

86. Cirulli ET, Lasseigne BN, Petrovski S, Sapp PC, Dion PA, Leblond CS, et al. Exome sequencing in amyotrophic lateral sclerosis identifies risk genes and pathways. Science. 2015 feb; 347(6229):1436–1441. Available from: http://www.sciencemag.org/content/347/6229/1436.full. doi: 10.1126/science.aaa3650 PMID: 25700176

87. Thornton KR. A C++ Template Library for Efficient Forward-Time Population Genetic Simulation of Large Populations. Genetics. 2014;(2013):1–21. Available from: http://www.ncbi.nlm.nih.gov/pubmed/24950894. doi: 10.1534/genetics.114.165019 PMID: 24950894

88. Kimura M. The number of heterozygous nucleotide sites maintained in a finite population due to steady flux of mutations. Genetics. 1969; 61(694):893–903. PMID: 5364968

89. Slatkin M. Heritable variation and heterozygosity under a balance between mutations and stabilizing selection. Genetical research. 1987; 50:53–62. doi: 10.1017/S0016672300023338 PMID: 3653689

90. Gravel S. When Is Selection Effective? Genetics. 2016 may; 203(1):451–62. Available from: http://www.ncbi.nlm.nih.gov/pubmed/27010021http://www.pubmedcentral.nih.gov/articlerender.fcgi?artid=PMC4858791. doi: 10.1534/genetics.115.184630 PMID: 27010021

91. Balick DJ, Do R, Cassa CA, Reich D, Sunyaev SR. Dominance of Deleterious Alleles Controls the Response to a Population Bottleneck. PLoS genetics. 2015 aug; 11(8):e1005436. Available from: http://journals.plos.org/plosgenetics/article?id=10.1371/journal.pgen.1005436. doi: 10.1371/journal.pgen.1005436 PMID: 26317225

92. Lumley T. biglm: bounded memory linear and generalized linear models; 2013. R package version 0.9-1. Available from: http://CRAN.R-project.org/package=biglm.

93. Haseman JK, Elston RC. The investigation of linkage between a quantitative trait and a marker locus. Behavior Genetics. 1972 mar; 2(1):3–19. Available from: http://link.springer.com/10.1007/BF01066731. doi: 10.1007/BF01066731 PMID: 4157472

94. Sham PC, Purcell S. Equivalence between Haseman-Elston and variance-components linkage analyses for sib pairs. American journal of human genetics. 2001 jun; 68(6):1527–32. Available from: http://www.pubmedcentral.nih.gov/articlerender.fcgi?artid=1226141&tool=pmcentrez&rendertype=abstract. doi: 10.1086/320593 PMID: 11353401

95. Purcell S, Neale B, Todd-Brown K, Thomas L, Ferreira MAR, Bender D, et al. PLINK: a tool set for whole-genome association and population-based linkage analyses. American journal of human genetics. 2007 sep; 81(3):559–75. Available from: http://www.sciencedirect.com/science/article/pii/S0002929707613524. doi: 10.1086/519795 PMID: 17701901

96. R Core Team. R: A Language and Environment for Statistical Computing. Vienna, Austria; 2014. Available from: http://www.R-project.org/.

97. Neale MC, Hunter MD, Pritikin JN, Zahery M, Brick TR, Kickpatrick RM, et al. OpenMx 2.0: Extended structural equation and statistical modeling. Psychometrika. in press; doi: 10.1007/s11336-014-9435-8 PMID: 25622929

98. McCarthy MI, Hirschhorn JN. Genome-wide association studies: Potential next steps on a genetic journey. Human Molecular Genetics. 2008; 17(2):156–165. doi: 10.1093/hmg/ddn289 PMID: 18852205

99. Marth GT, Czabarka E, Murvai J, Sherry ST. The Allele Frequency Spectrum in Genome-Wide Human Variation Data Reveals Signals of Differential Demographic History in Three Large World Populations. Genetics. 2004; 166(1):351–372. doi: 10.1534/genetics.166.1.351 PMID: 15020430